Short Article

Cell Metabolism

Mitochondrial OXA Translocase Plays a Major Role in Biogenesis of Inner-Membrane Proteins

Graphical Abstract

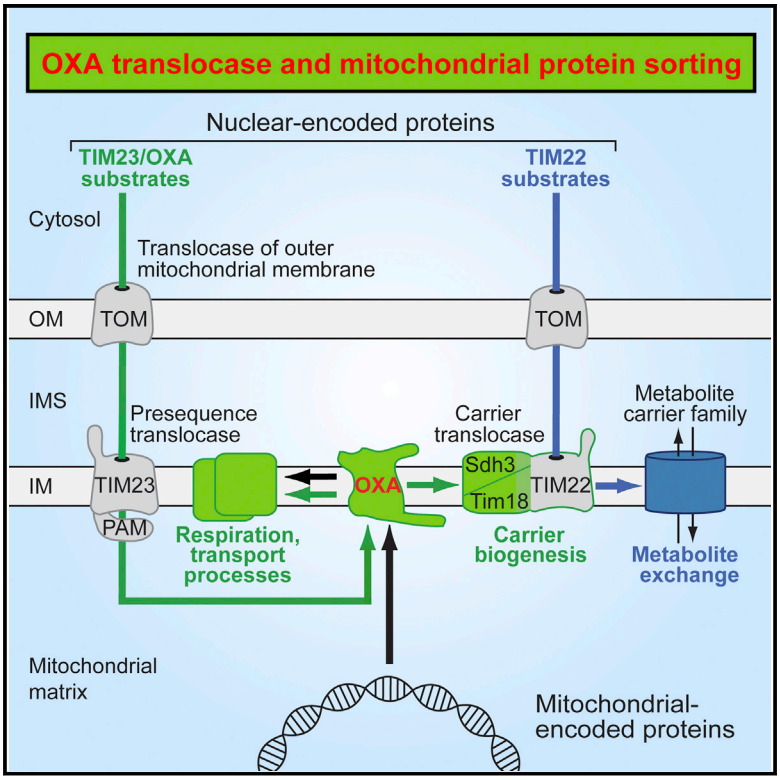

Highlights

- Systematic search for substrates of mitochondrial inner-membrane OXA translocase
- OXA translocase has different functions in presequence and carrier pathways
- Many cleavable preproteins use the presequence translocase-OXA import-export pathway
- OXA promotes carrier import via assembly of Tim18-Sdh3 module of carrier translocase

Authors

Sebastian B. Stiller, Jan Höpker, Silke Oeljeklaus, ..., Bettina Warscheid, Nikolaus Pfanner, Nils Wiedemann

Correspondence

nikolaus.pfanner@biochemie.uni-freiburg.de (N.P.), nils.wiedemann@biochemie.uni-freiburg.de (N.W.)

In Brief

Stiller et al. report that the sorting of many nuclear-encoded mitochondrial proteins depends on the OXA translocase, a homolog of bacterial YidC. The conservative sorting of transmembrane segments into the mitochondrial inner membrane is required for assembly of the carrier translocase and thus for the biogenesis of numerous metabolite carriers.

Stiller et al., 2016, Cell Metabolism *23*, 901–908
May 10, 2016
http://dx.doi.org/10.1016/j.cmet.2016.04.005

CellPress

Cell Metabolism
Short Article

Mitochondrial OXA Translocase Plays a Major Role in Biogenesis of Inner-Membrane Proteins

Sebastian B. Stiller,[1,2,6] Jan Höpker,[1,2,6] Silke Oeljeklaus,[3,4] Conny Schütze,[1] Sandra G. Schrempp,[1,2] Jens Vent-Schmidt,[1,7] Susanne E. Horvath,[1] Ann E. Frazier,[1,8] Natalia Gebert,[1] Martin van der Laan,[1,4,5] Maria Bohnert,[1,9] Bettina Warscheid,[3,4] Nikolaus Pfanner,[1,4,*] and Nils Wiedemann[1,4,*]
[1]Institute of Biochemistry and Molecular Biology, ZBMZ, Faculty of Medicine
[2]Faculty of Biology
[3]Institute of Biology II, Biochemistry – Functional Proteomics, Faculty of Biology
[4]BIOSS Centre for Biological Signalling Studies
University of Freiburg, 79104 Freiburg, Germany
[5]Medical Biochemistry and Molecular Biology, Saarland University, 66421 Homburg, Germany
[6]Co-first author
[7]Present address: Department of Surgery, University of British Columbia, Vancouver, BC V5Z 1M9, Canada; Child and Family Research Institute, Vancouver, BC V5Z 4H4, Canada
[8]Present address: Murdoch Childrens Research Institute, Royal Children's Hospital and Department of Paediatrics, University of Melbourne, 3052 Melbourne, Australia
[9]Present address: Department of Molecular Genetics, Weizmann Institute of Science, Rehovot 7610001, Israel
*Correspondence: nikolaus.pfanner@biochemie.uni-freiburg.de (N.P.), nils.wiedemann@biochemie.uni-freiburg.de (N.W.)
http://dx.doi.org/10.1016/j.cmet.2016.04.005

SUMMARY

The mitochondrial inner membrane harbors three protein translocases. Presequence translocase and carrier translocase are essential for importing nuclear-encoded proteins. The oxidase assembly (OXA) translocase is required for exporting mitochondrial-encoded proteins; however, different views exist about its relevance for nuclear-encoded proteins. We report that OXA plays a dual role in the biogenesis of nuclear-encoded mitochondrial proteins. First, a systematic analysis of OXA-deficient mitochondria led to an unexpected expansion of the spectrum of OXA substrates imported via the presequence pathway. Second, biogenesis of numerous metabolite carriers depends on OXA, although they are not imported by the presequence pathway. We show that OXA is crucial for the biogenesis of the Tim18-Sdh3 module of the carrier translocase. The export translocase OXA is thus required for the import of metabolite carriers by promoting assembly of the carrier translocase. We conclude that OXA is of central importance for the biogenesis of the mitochondrial inner membrane.

INTRODUCTION

The mitochondrial inner membrane is a protein-rich membrane harboring the respiratory chain complexes and numerous metabolite carriers. Two genetic systems are required for formation of the inner membrane (Neupert and Herrmann, 2007; Chacinska et al., 2009; Endo and Yamano, 2009). The mitochondrial genome encodes a small number of proteins. These typically hydrophobic proteins are synthesized in the mitochondrial matrix and are exported into the inner membrane by the cytochrome oxidase assembly (OXA) translocase (Hell et al., 2001; Funes et al., 2011). Oxa1, the major component of the OXA translocase, has been conserved from the prokaryotic ancestor of mitochondria and is thought to function as a membrane protein insertase like prokaryotic YidC (Hell et al., 2001; Funes et al., 2011; Kumazaki et al., 2014). Cox18 (Oxa2), an Oxa1 paralog, plays a minor role in the export of mitochondrial-encoded proteins (Funes et al., 2004; Bonnefoy et al., 2009).

Most inner-membrane proteins, however, are encoded by nuclear genes and are synthesized as precursors on cytosolic ribosomes. Targeting signals direct these precursor proteins to mitochondria and into the inner membrane. Two major classes of inner-membrane precursor proteins can be distinguished (Neupert and Herrmann, 2007; Chacinska et al., 2009). Preproteins transported by the presequence translocase of the inner membrane (TIM23 complex) typically carry cleavable amino-terminal targeting signals. These positively charged presequences are removed by the mitochondrial processing peptidase (MPP) in the matrix. Precursor proteins transported by the carrier translocase of the inner membrane (TIM22 complex) do not contain cleavable presequences, but internal targeting signals distributed over the mature part of the protein. Presequence translocase and carrier translocase are activated by the membrane potential ($\Delta\psi$) across the inner membrane to drive translocation of precursor proteins.

Whereas all precursors known to be imported by the carrier translocase are laterally released into the inner membrane, two distinct pathways are possible with the presequence translocase. (1) Cleavable preproteins with hydrophobic stop transfer signals are arrested during translocation by the TIM23 complex and are laterally released into the lipid phase of the inner membrane (Glick et al., 1992; Botelho et al., 2011; Park et al., 2013; Ieva et al., 2014). (2) The presequence translocase-associated motor (PAM) cooperates with the TIM23 complex in the import

A

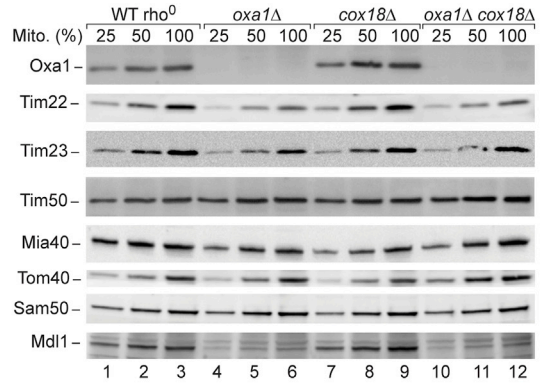

B

ORF	Protein name	Pre-sequence	Predicted TM segments	Description
YMR301C	Atm1	+	6	ABC Transporters
YPL270W	Mdl2	+	6	
YPL224C	Mmt2	+	5	Metal Transporter
YNR041C	Coq2	+	5	Ubiquinone Biosynthesis
YDL217C	Tim22	–	4	Protein Translocase
YKL141W	Sdh3	+	3	Succinat Dehydrogenase
YDR178W	Sdh4	+	3	
YDL085W	Nde2	+	3	External NADH Dehydrogenase
YEL052W	Afg1	+	3	AAA protein
YNR018W	Rcf2	–	2	Respiratory Chain Assembly
YER141W	Cox15	+	2	
YCL057C-A	Mic10	–	2	MICOS
YKR065C	Pam17	+	2	Protein Translocase
YBL030C	Aac2	–	6	Metabolite Carriers
YOR100C	Crc1	–	6	
YOR271C	Fsf1	–	6	
YDL198C	Ggc1	–	6	
YJR077C	Mir1	–	6	
YKL120W	Oac1	–	6	
YPL134C	Odc1	–	6	
YOR222W	Odc2	–	6	
YOR130C	Ort1	–	6	
YNL003C	Pet8	–	6	
YER053C	Pic2	–	6	
YBR192W	Rim2	–	6	
YMR241W	Yhm2	–	6	
YPR058W	Ymc1	–	6	
YBR104W	Ymc2	–	6	

Figure 1. Mitochondrial Inner-Membrane Proteins Affected in OXA-Deficient Yeast Mutants

(A) The levels of translocase core subunits and of Mdl1 of wild-type (WT) rho^0, *oxa1Δ*, *cox18Δ*, and *oxa1Δ cox18Δ* mitochondria were analyzed by SDS-PAGE and immunoblotting. Mito., total mitochondrial protein; 100% represents 40 μg protein (80 μg for Sam50).

(B) Differential analysis of the proteome of WT rho^0 compared to *oxa1Δ cox18Δ* mitochondria using MS. WT rho^0 and *oxa1Δ cox18Δ* cells were differentially labeled with stable isotopes, mixed and mitochondria were isolated and analyzed by quantitative MS (Table S1). Integral inner-membrane proteins found to be depleted in *oxa1Δ cox18Δ* mitochondria (heavy/light ratio >1.6) are listed with the yeast open reading frame (ORF).

See also Figure S1, and Table S1, and Table S2.

of preproteins into the matrix. The mitochondrial heat shock protein 70 (mtHsp70, Ssc1) is the core component of PAM and drives matrix translocation of proteins in an ATP-dependent manner (Neupert and Herrmann, 2007; Chacinska et al., 2009). The TIM23-PAM pathway is obligatory for the import of all matrix proteins; however, it is also used by a few inner-membrane proteins. Upon import into the matrix, these inner-membrane precursors are exported into the membrane by the OXA translocase. This import-export pathway was termed the conservative sorting pathway, since the OXA-dependent protein export has been conserved from the prokaryotic ancestor of mitochondria (Neupert and Herrmann, 2007). To date, however, only three authentic nuclear-encoded proteins were shown to be exported by the OXA translocase in yeast: the precursors of Oxa1 and Cox18 themselves and the ABC transporter Mdl1 (Herrmann et al., 1997; Hell et al., 1998; Funes et al., 2004; Bohnert et al., 2010). Additionally, the Rieske Fe/S protein follows an import-export pathway, yet uses the AAA-ATPase Bcs1 as a precursor-specific export and assembly machine instead of the OXA translocase (Hartl et al., 1986; Wagener et al., 2011). The available data thus support the view that the vast majority of cleavable inner-membrane proteins are not sorted via OXA, but are laterally released from the TIM23 complex by a stop transfer mechanism (Glick et al., 1992; Neupert and Herrmann, 2007; Bohnert et al., 2010; Ieva et al., 2014).

Hildenbeutel et al. (2012) reported that Oxa1 is involved in the biogenesis of several metabolite carriers that are imported by the TIM22 complex. Since carrier precursors are inserted into the inner membrane from the intermembrane space side and are not translocated into the matrix (Neupert and Herrmann, 2007; Chacinska et al., 2009), the role of OXA cannot be explained by an export of the precursors from the matrix. It was discussed that OXA may promote the folding of imported carrier proteins or influence the lipid composition of the inner membrane (Hildenbeutel et al., 2012).

Here we identified numerous nuclear-encoded mitochondrial proteins that depend on OXA and establish the OXA translocase as a major machinery for the biogenesis of the inner membrane. OXA is also required for the biogenesis of the Tim18-Sdh3 module of the TIM22 carrier translocase, explaining the disturbed carrier import in OXA-deficient mitochondria.

RESULTS AND DISCUSSION

Mitochondrial Inner-Membrane Proteins Depleted in OXA-Deficient Mitochondria

To study a possible influence of OXA on other preprotein translocases, we analyzed the protein levels in *oxa1Δ* mitochondria, *cox18Δ* mitochondria, and *oxa1Δ cox18Δ* mitochondria from budding yeast. The levels of Tim22 were reduced in *oxa1Δ* mitochondria and *oxa1Δ cox18Δ* mitochondria, whereas other protein import machineries, including presequence translocase (Tim23, Tim50), mitochondrial intermembrane space import and assembly machinery (Mia40), translocase of outer membrane (Tom40), and sorting and assembly machinery (Sam50), were not or were only mildly affected (Figure 1A). For comparison, the levels of the known Oxa1 substrate Mdl1 (Bohnert et al., 2010) were considerably reduced in *oxa1Δ* and *oxa1Δ cox18Δ* mitochondria.

A connection of OXA to the TIM22 complex could provide an explanation for its influence on the import of metabolite carriers (Hildenbeutel et al., 2012). So far, however, neither OXA nor any of the known OXA substrates have been linked to the TIM22 translocase. We performed a systematic approach to screen for mitochondrial inner-membrane proteins depleted in OXA-deficient mitochondria. We used a quantitative mass spectrometry (MS)-based approach to compare *oxa1*Δ *cox18*Δ mitochondria and control mitochondria. Since Oxa1-deficient mitochondria are strongly impaired in protein complexes containing mitochondrial-encoded subunits, including oxidative phosphorylation complexes III, IV, and V (see Figure S1 available online), the levels of many subunits of these complexes can be decreased independently if they are OXA substrates or not (Bonnefoy et al., 2009). Thus, wild-type mitochondria containing a functional mitochondrial genome (rho$^+$) do not represent an appropriate control for *oxa1*Δ *cox18*Δ mitochondria. We found that wild-type rho^0 mitochondria, which lack mtDNA but contain Oxa1 and Cox18, represented the most stringent control for screening for OXA-substrates. Wild-type rho^0 cells and *oxa1*Δ *cox18*Δ cells were differentially labeled with stable isotopes and mixed, and isolated mitochondria were subjected to MS analysis (Table S1). Mitochondrial inner-membrane proteins depleted in *oxa1*Δ *cox18*Δ mitochondria are listed in Figure 1B. Tim22 was depleted in agreement with the analysis of its steady-state levels by immunodecoration (Figure 1A). We identified many members of the metabolite carrier family, and further noncleavable proteins (Mic10, Rcf2), as well as numerous cleavable proteins, including the ABC transporters Atm1 and Mdl2, the metal transporter Mmt2, and Sdh3 and Sdh4 of respiratory complex II (succinate dehydrogenase [SDH]) (Figure 1B). Thus, a broad spectrum of inner-membrane proteins were depleted in OXA-deficient mitochondria.

Oxa1 Is Required for Assembly of Both SDH Complex and TIM22 Complex

All subunits of the metazoan and fungal SDH complex are nuclear encoded. The membrane-integrated module Sdh3-Sdh4 is evolutionarily related to the Sdh3-Tim18 module of the TIM22 complex. Tim18 is a paralog of Sdh4, and Sdh3 is a subunit of both the SDH complex and the TIM22 complex (Gebert et al., 2011). Immunodecoration revealed that all three proteins were strongly depleted in *oxa1*Δ mitochondria and *oxa1*Δ *cox18*Δ mitochondria, but not in *cox18*Δ mitochondria (Figure 2A). The level of Sdh1 of the hydrophilic matrix-exposed portion of the SDH complex was only mildly affected in the mutant mitochondria. Similarly, the levels of the intermembrane space-exposed proteins of the TIM22 complex, Tim54 and Tim9-Tim10-Tim12, were close to that of control mitochondria (Figure 2A), whereas the levels of Tim22 were moderately reduced upon deletion of *OXA1* (Figures 1A and 2A). The mature assembled SDH complex and TIM22 complex were analyzed by blue native electrophoresis of digitonin-lysed mitochondria. Consistent with the depletion of crucial subunits, the levels of the mature complexes were strongly decreased in Oxa1-deficient mitochondria (Figure 2B).

To discriminate between direct and indirect Oxa1 effects, we used a temperature-sensitive *oxa1* yeast mutant. Upon growth of the mutant cells at permissive temperature, the levels of mitochondrial proteins were not or were only mildly affected in comparison to rho$^+$ wild-type mitochondria (Figures S2A and S2B). The Oxa1 defect was induced by a short in vitro heat shock (12 min 37°C) of isolated *oxa1-ts* mitochondria (Hell et al., 2001; Preuss et al., 2001; Bohnert et al., 2010), leading to a degradation of the OXA complex (Figure S3A). The steady levels of other protein complexes including SDH and TIM22 were not affected by the in vitro heat shock (Figure S3A). To test the Oxa1 function in a kinetic range, we imported the ^{35}S-labeled precursor of Tim18 into isolated energized mitochondria. Upon the in vitro heat shock, assembly of Tim18 into the TIM22 complex as well as formation of the Tim18-Sdh3 assembly intermediate (Gebert et al., 2011) was strongly impaired in *oxa1-ts* mitochondria (Figure 2C; Figures S3B and S3C). Similarly, the assembly of Sdh4 into the mature SDH complex and formation of the Sdh3-Sdh4 assembly intermediate (Gebert et al., 2011) were inhibited (Figure 2D; Figure S3D). Translocation to a protease-protected location and processing were not or were only mildly affected in heat-shocked *oxa1-ts* mitochondria, as shown for Tim18, Sdh3, and matrix-targeted preproteins (Figures S3E and S3F), indicating that functional Oxa1 is not crucial for the initial translocation into mitochondria. Upon import into mitochondria, the ^{35}S-labeled precursor of Sdh4, but not fully assembled endogenous Sdh4, was copurified with tagged Oxa1 (Figure S3G). Taken together, we conclude that Oxa1 plays a specific role in the assembly pathways of Tim18, Sdh3, and Sdh4.

Δψ-dependent import and assembly of metabolite carriers were monitored by blue native electrophoresis (Gebert et al., 2011). Upon import of the ^{35}S-labeled precursors of ADP/ATP carrier (Aac2) and dicarboxylate carrier (Dic1) into heat-shocked *oxa1-ts* mitochondria, their assembly was indistinguishable from that of wild-type mitochondria (Figure 2E). Hildenbeutel et al. (2012) showed, however, that the levels of Aac2 were diminished in *oxa1*Δ mitochondria and that the import of carrier precursors was reduced in Oxa1-depleted mitochondria (isolated from *oxa1* mutant cells that had been heat shocked for 3 hr). Our analysis of *oxa1*Δ mitochondria agrees with the findings of Hildenbeutel et al. (2012). The levels of metabolite carriers analyzed by immunoblotting were reduced (Figure 2F), in agreement with the depletion of numerous metabolite carriers in the MS analysis (Figure 1B; Table S1). Assembly of ^{35}S-labeled Dic1 was strongly inhibited in *oxa1*Δ mitochondria in comparison to wild-type mitochondria (rho$^+$ as well as rho^0 wild-type) (Figure 2G). Thus, the in vitro induction of the *oxa1-ts* mutant phenotype by a short heat shock of isolated mitochondria provides the basis for separating direct and indirect effects of Oxa1 on mitochondrial protein biogenesis. The assembly pathways of Tim18, Sdh3, and Sdh4, but not of metabolite carriers, directly depend on functional Oxa1. Since a defective assembly of the TIM22 complex impairs subsequent import of metabolite carriers (Gebert et al., 2011), depletion of Oxa1 will lead to defects in the biogenesis of carrier proteins.

Differential Roles of Import Motor and OXA in the Sorting of Sdh4/Sdh3/Tim18

Since OXA exports polypeptides from the matrix, nuclear-encoded polypeptides that directly depend on OXA have to be translocated into the matrix. The mtHsp70 import motor PAM is essential for protein translocation into the matrix (Neupert

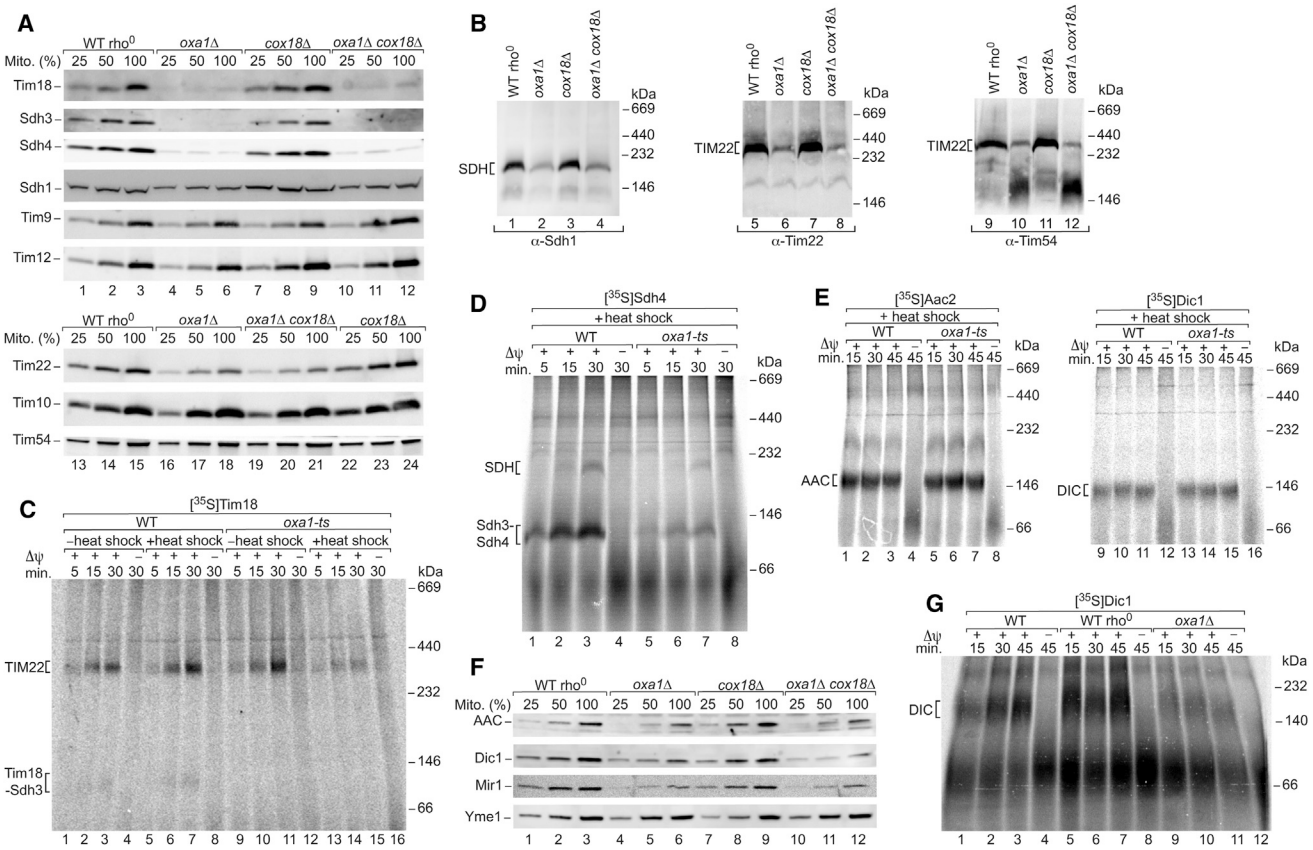

Figure 2. Oxa1-Dependent Assembly of SDH Complex and TIM22 Complex

(A) Protein levels of TIM22 and SDH subunits were analyzed in the indicated mitochondria by SDS-PAGE and immunoblotting. Mito., total mitochondrial protein; 100% represents 160 μg protein (40 μg for Sdh3 and Sdh4; 80 μg for Tim9 and Tim12).

(B) SDH complex and TIM22 complex were analyzed by blue native electrophoresis of isolated mitochondria and immunoblotting.

(C) Mitochondria were either heat shocked for 12 min at 37°C or incubated at 25°C, followed by import of [^{35}S]Tim18 precursor at 25°C. After Proteinase K treatment, assembly into the TIM22 complex was monitored by blue native electrophoresis and autoradiography.

(D) After an in vitro heat shock of mitochondria, [^{35}S]Sdh4 precursor was imported at 30°C, followed by Proteinase K treatment. Assembly of SDH and the Sdh3-Sdh4 intermediate were analyzed by blue native electrophoresis.

(E) Mitochondria were subjected to a heat shock, followed by import of [^{35}S]Aac2 and [^{35}S]Dic1 at 25°C and Proteinase K treatment. Carrier assembly was monitored by blue native electrophoresis.

(F) Protein levels were analyzed by SDS-PAGE and immunoblotting. Mito., total mitochondrial protein; 100% represents 40 μg protein.

(G) Dic1 was imported into mitochondria. After Proteinase K treatment, carrier assembly was monitored by blue native electrophoresis.

See also Figures S2 and S3 and Table S2.

and Herrmann, 2007; Chacinska et al., 2009). We asked if the dependence on PAM differed for the import pathways of Sdh4/Sdh3/Tim18 and metabolite carriers, similar to their differential dependence on functional Oxa1. We used temperature-sensitive yeast mutants of mtHsp70 (*ssc1-3*) and the cochaperone Pam16 (*pam16-3*). Isolated mitochondria were subjected to a short in vitro heat shock (12–15 min, 37°C) and incubated with the ^{35}S-labeled preproteins. The biogenesis pathways of Sdh4/Sdh3/Tim18 were blocked in *ssc1-3* mitochondria and diminished in *pam16-3* mitochondria (Figures 3A and 3B; Figure S4A). In contrast, the biogenesis pathways of Aac2 and Dic1 were neither inhibited in *ssc1-3* nor in *pam16-3* mitochondria (Figure 3C), supporting the conclusion that Sdh4/Sdh3/Tim18 and metabolite carriers use different sorting routes.

Sdh4, Sdh3, and Tim18 each contain three transmembrane segments (TMs); the N termini are exposed to the matrix and the C termini to the intermembrane space (Sun et al., 2005; Huang et al., 2006; Gebert et al., 2011). We observed that the C-terminal segment of Sdh4 was accessible to protease from the intermembrane space side and used this assay to probe the insertion of [^{35}S]Sdh4 into the inner membrane (Figure 3D; Figure S4B). The precursor of Sdh4 was imported in a Δψ-dependent manner and processed to the mature form, which was protected against Proteinase K added to the isolated mitochondria (Figure 3D, lane 2). Upon opening of the outer membrane by swelling of mitochondria, Proteinase K generated a truncated form Sdh4′ that was ~3 kDa smaller (Figure 3D, lane 5), consistent with the removal of the ~28-residue C-terminal segment that is located behind TM3 (TM1 and TM2 are connected by a short ~5-residue loop that is not accessible to the protease; Sun et al., 2005). With heat-shocked *ssc1-3* mitochondria, Sdh4 was processed to the mature-sized protein; however,

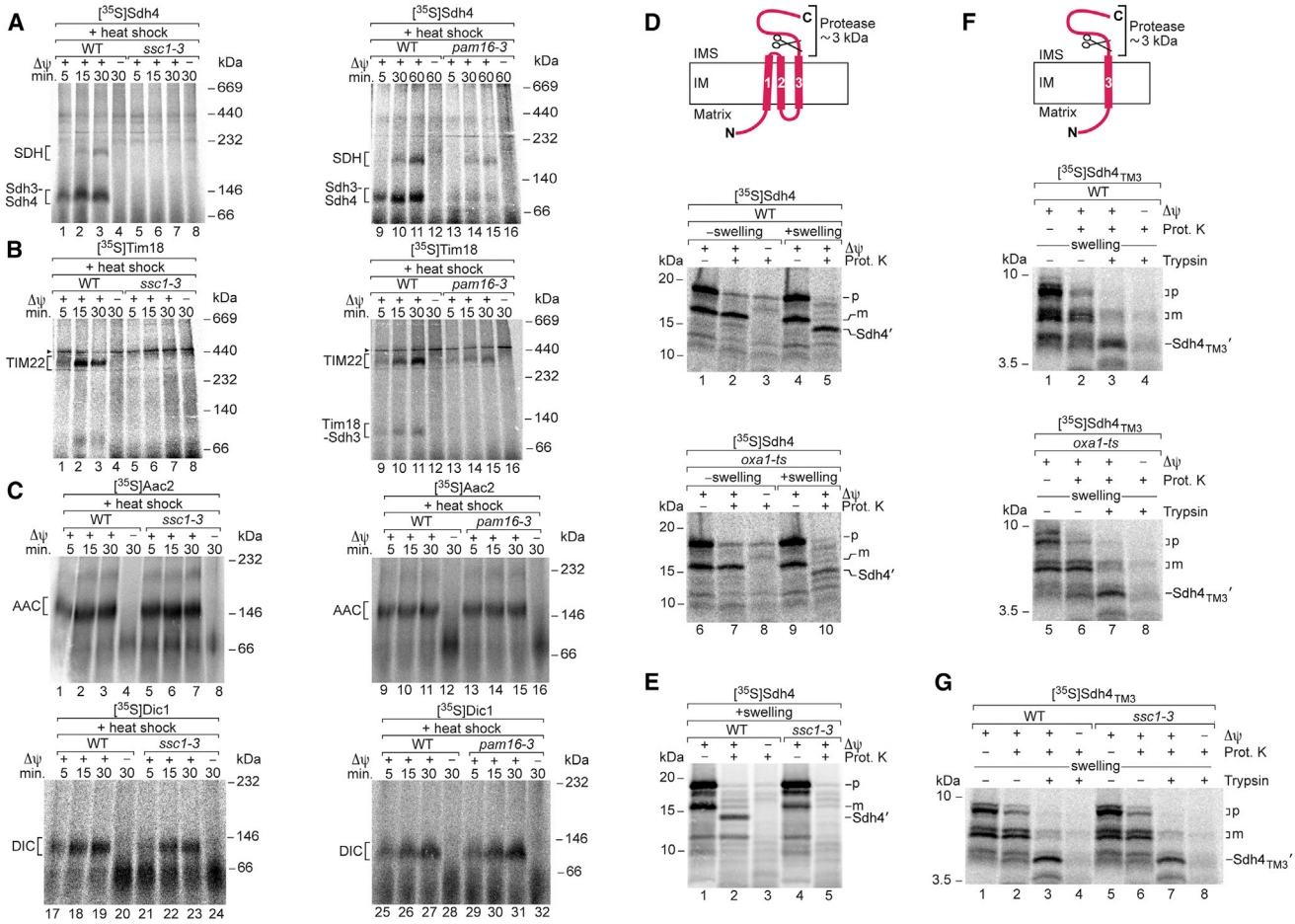

Figure 3. Mitochondrial Sorting of Sdh4 and Tim18 Depends on the mtHsp70 Import Motor

(A–C) Import of ^{35}S-labeled Sdh4 (A), Tim18 (B), Aac2 and Dic1 (C) into in vitro heat-shocked (37°C for 12–15 min) wild-type (WT), *ssc1-3*, and *pam16-3* mitochondria at 25°C (30°C for A, lanes 1–8), followed by Proteinase K treatment. Arrowhead, unspecific band.

(D–G) ^{35}S-labeled Sdh4 (D and E) or TM3 fused to the Sdh4 presequence, [^{35}S]Sdh4$_{TM3}$ (F and G), were imported into WT, *oxa1-ts*, and *ssc1-3* mutant mitochondria at 30°C. WT and mutant mitochondria were heat shocked prior to the import reaction. Nonimported [^{35}S]Sdh4$_{TM3}$ was removed by Proteinase K treatment. After washing, mitochondria were suspended in either isotonic buffer (−swelling) or hypotonic buffer (+swelling). Where indicated, Proteinase K or trypsin was added. The mitochondrial samples were analyzed by SDS-PAGE and autoradiography. p, precursor; m, mature form; Sdh4′ and Sdh4$_{TM3}$′, protease-protected Sdh4 and Sdh4$_{TM3}$ fragments. Cartoons in (D) and (F): the TMs of Sdh4 are numbered from 1 to 3; IM, inner membrane; IMS, intermembrane space. See also Figure S4 and Table S2.

formation of the truncated Sdh4′ form was blocked (Figure 3E), demonstrating that an active motor was required to drive efficient import of the mature portion of Sdh4. In contrast, with heat-shocked *oxa1-ts* mitochondria, truncated Sdh4′ was formed (Figure 3D, lane 10), indicating that a functional Oxa1 was not crucial for membrane insertion of the C-terminal TM3.

How can these differential effects of mtHsp70 and Oxa1 on the sorting of Sdh4 be explained? A comparison of TMs of mitochondrial inner-membrane proteins suggested that TMs arrested in the inner membrane by a stop transfer mechanism are more hydrophobic than TMs imported into the matrix; a proline residue in a TM also favors translocation into the matrix (Meier et al., 2005; Botelho et al., 2011; Park et al., 2013, 2014). Park et al. (2013) analyzed membrane insertion of the TMs of Sdh4 in the context of fusion proteins and suggested that TM1 (containing a proline residue) and TM2 are translocated into the matrix, whereas TM3 is probably arrested in the inner membrane. Figure S4C presents a model that combines the analysis of TMs and our findings on the differential dependence on mtHsp70 and OXA: the motor PAM is required to drive import of the N-terminal portion of Sdh4 including TM1 and TM2 for subsequent export by OXA, whereas TM3 is arrested in the TIM23 complex by a stop-transfer mechanism and laterally released into the membrane in an OXA-independent manner.

To directly test the predicted independence of TM3 from mtHsp70 and OXA, we generated a shortened form of Sdh4 that lacked TM1 and TM2 but contained the presequence plus TM3 and the C-terminal segment (Figure S4B). ^{35}S-labeled Sdh4$_{TM3}$ was imported into mitochondria in a Δψ-dependent manner and processed to the mature-sized form. m-Sdh4$_{TM3}$ was protected against protease added to mitochondria but cleaved to the truncated form Sdh4$_{TM3}$′ upon opening of the

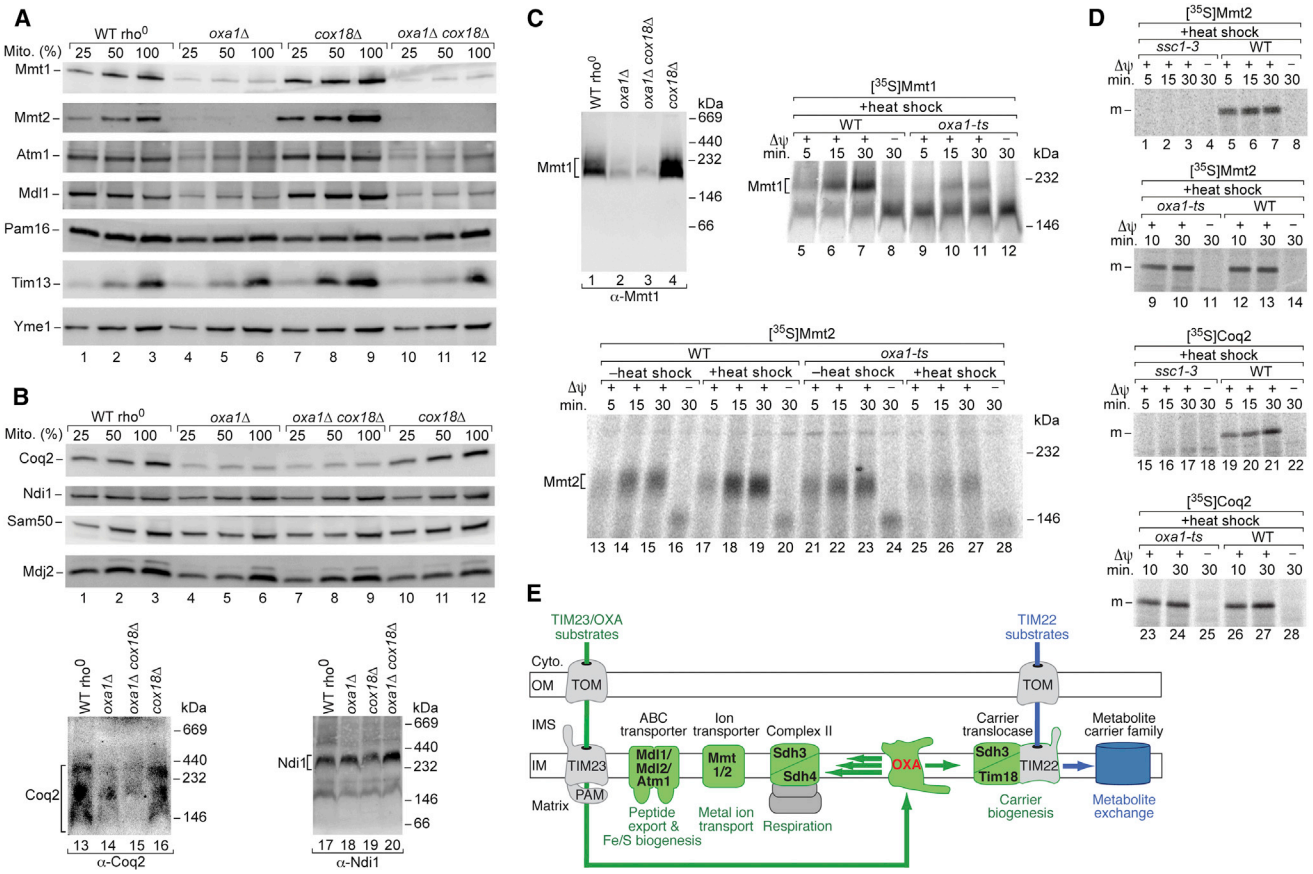

Figure 4. Role of OXA in the Biogenesis of Nuclear-Encoded Inner-Membrane Proteins

(A and B) Mitochondria isolated from the indicated yeast cells were either subjected to SDS-PAGE or lysed with 1% digitonin and analyzed by blue native electrophoresis, followed by immunoblotting. Mito., total mitochondrial protein; 100% represents 160 μg protein (40 μg for Tim13 and Yme1; 80 μg for Atm1 and Mdl1; 320 μg for Ndi1).

(C) Samples 1–4, the indicated mitochondria were lysed with digitonin and analyzed by blue native electrophoresis and immunoblotting. Samples 5–28, mitochondria were subjected to a heat shock where indicated; Mmt1 and Mmt2 were imported, followed by Proteinase K treatment. Mitochondria were analyzed by blue native electrophoresis and autoradiography.

(D) Heat-treated (15 min 37°C) mitochondria were incubated with Mmt2 or Coq2 precursors at 25°C, followed by Proteinase K treatment and SDS-PAGE.

(E) Model of Oxa1 function in the biogenesis of nuclear-encoded mitochondrial inner-membrane proteins. Cyto., cytosol; OM, outer membrane; IMS, intermembrane space; IM, inner membrane.

See also Figure S4.

outer membrane (Figure 3F, upper panel). Truncated $Sdh4_{TM3}'$ was similarly generated with *ssc1-3* mitochondria (Figure 3G) as well as *oxa1-ts* mitochondria (Figure 3F, lower panel), demonstrating that both functional mtHsp70 and Oxa1 were dispensable for import and inner-membrane sorting of TM3. $Sdh4_{TM3}$ thus fulfills all requirements for sorting via a stop transfer mechanism (Figure S4D). Taken together with the study by Park et al. (2013), we conclude that the biogenesis of Sdh4 involves two sorting pathways: mtHsp70-dependent import into the matrix and OXA-mediated export for TM1 and TM2, as well as stop transfer and lateral release into the inner membrane for TM3 (Figure S4C).

Major Role of OXA in the Biogenesis of Inner-Membrane Proteins

To further assess the importance of OXA for the biogenesis of nuclear-encoded inner-membrane proteins, we subjected additional candidate proteins derived from the MS analysis (Figure 1B) to a biochemical analysis. We tested proteins with lower MS intensities in *oxa1*Δ *cox18*Δ mitochondria as well as proteins belonging to the same protein family, including: the mitochondrial metal transporters Mmt1 and Mmt2, which are involved in mitochondrial iron accumulation; the ABC transporters Atm1 and Mdl1; and Coq2, an inner-membrane polyprenyl transferase functioning in the biosynthesis of ubiquinone. The levels of these proteins were considerably decreased in *oxa1*Δ mitochondria and *oxa1*Δ *cox18*Δ mitochondria (Figures 4A and 4B) in agreement with the MS findings and the reported OXA-dependence of Mdl1 (Bohnert et al., 2010; Figure 1A). Blue native analysis using *oxa1-ts* mitochondria showed that the assembly pathways of Mmt1 and Mmt2 depended on functional Oxa1 (Figure 4C; Figure S4E). To obtain further evidence that a conservative sorting pathway was used, we studied the initial import of Mmt2 and Coq2 to a protease-protected location. Both precursors contain

proline within the predicted TMs, favoring translocation into the matrix (Meier et al., 2005). Indeed, the initial import strictly depended on functional mtHsp70, yet not Oxa1 (Figure 4D). The ^{35}S-labeled precursor of Mmt2, but not mature endogenous Mmt2, was copurified with tagged Oxa1 (Figure S4F), strongly supporting an OXA-mediated sorting. Various inner-membrane control proteins did not reveal a dependence on OXA, including the AAA protease Yme1, the internal NADH dehydrogenase Ndi1 and the motor subunit Mdj2 (Figures 4A and 4B; Table S1).

Thus, the MS-based depletion study represents an important source for finding mitochondrial inner-membrane proteins that depend on OXA, leading to the discovery of numerous nuclear-encoded substrates of the OXA export translocase. Since to date only Oxa1/Cox18 and Mdl1 have been known as authentic nuclear-encoded OXA substrates, this represents a major expansion of the role of OXA in inner-membrane biogenesis. However, two important points have to be considered. (1) The MS analysis reported here only represents a screening approach, and thus a biochemical analysis of inner-membrane sorting and assembly is required to define the molecular mechanisms of an OXA involvement. This is most evident in the case of the metabolite carriers of the inner membrane. The biogenesis pathway of carrier precursors is compromised in Oxa1-depleted mitochondria (Hildenbeutel et al., 2012; this study); however, not by a direct function of Oxa1 in carrier sorting and folding. We found that Oxa1 is crucial for the assembly pathway of the Tim18-Sdh3 module of the TIM22 carrier translocase, demonstrating that the export translocase is required for the proper assembly of this import translocase (Figure 4E). (2) To minimize false-positive identifications of OXA-dependent proteins, we used strict criteria for selecting the control mitochondria. It is thus conceivable that the number of OXA-dependent inner-membrane proteins is even larger. This is exemplified by the biochemical identification of OXA substrates such as Tim18, Mdl1, and Mmt1, which were not found by the MS analysis, but are related to proteins identified in the study.

The TIM23, PAM, and OXA machineries show a high versatility in the sorting of mitochondrial inner-membrane proteins. In the case of Sdh4, the first two TMs use the PAM/OXA-dependent import-export pathway, whereas TM3 is laterally released from the TIM23 complex into the inner membrane via the PAM/OXA-independent stop-transfer pathway (Figure S4C). In contrast, in the case of Mdl1, an opposite order of the two sorting pathways was observed (Bohnert et al., 2010). Thus, depending on the characteristics of sorted preproteins, lateral sorting via TIM23 and conservative sorting via OXA can be combined sequentially in order to properly assemble inner-membrane proteins.

In summary, the OXA export translocase plays a central role in the biogenesis of the mitochondrial inner membrane. In addition to its well-established role in the export of mitochondrial-encoded proteins (Hell et al., 2001; Bonnefoy et al., 2009), OXA promotes the proper sorting of numerous nuclear-encoded proteins with multiple TMs by two different mechanisms (Figure 4E). Inner-membrane precursors/domains, which are imported into the matrix by the presequence translocase/mtHsp70 motor machinery (TIM23-PAM), are subsequently exported by OXA. The OXA substrates characterized here and in previous studies have been conserved from bacteria to mitochondria in line with a conservative sorting mechanism (Herrmann et al., 1997; Hell et al., 1998; Funes et al., 2004; Bohnert et al., 2010), whereas the available evidence suggests that the metabolite carrier family has a eukaryotic origin (Palmieri, 2013). The large number of metabolite carriers do not use the TIM23-PAM-OXA pathway; however, two subunits of the carrier translocase TIM22 use this pathway. Thus, in OXA-depleted mitochondria, biogenesis and activity of the carrier translocase are strongly inhibited.

EXPERIMENTAL PROCEDURES

Growth of Yeast and Isolation of Mitochondria

The *Saccharomyces cerevisiae* strains used in this study are listed in Table S2. Yeast cells were grown in YPS (1% [w/v] yeast extract, 2% [w/v] peptone, 2% [w/v] sucrose) or YPG (1% [w/v] yeast extract, 2% [w/v] peptone, 3% [v/v] glycerol) at 21°C or 30°C. Mitochondria were isolated by differential centrifugation and stored in SEM buffer (250 mM sucrose, 1 mM EDTA, 10 mM MOPS-KOH [pH 7.2]) at −80°C. For MS analysis, cells were cultured in minimal medium (0.67% [w/v] yeast nitrogen base without amino acids, 0.69 g/l of CSM-ARG-LYS dropout medium [MP Biomedicals] and 2% [w/v] sucrose) containing either [$^{13}C_6$/$^{15}N_2$]lysine and [$^{13}C_6$/$^{15}N_4$]arginine (Eurisotop) (for YPH499 rho^0) or natural lysine and arginine (for *oxa1Δ cox18Δ*; referred to as light amino acids). Cells were mixed in a ratio of 1:1 (based on their OD_{600}) prior to isolation of mitochondria.

Import of Precursor Proteins into Mitochondria

Template DNA-encoding mitochondrial precursor proteins were amplified from genomic *S. cerevisiae* DNA using forward primers containing an SP6 promoter and reverse primers that bind at the 3′ end of the respective open reading frames. mRNA was obtained by in vitro transcription using the mMessage mMachine kit (Ambion). For purification of mRNA, the MEGAclear kit (Ambion) was employed. ^{35}S-labeled proteins were synthesized in rabbit reticulocyte lysate (Promega) or wheat germ lysate (5 PRIME, for Mmt1). Import of radiolabeled precursor proteins into isolated yeast mitochondria was performed in the presence of 4 mM NADH, 4 mM ATP, and an ATP regenerating system (10 mM creatine phosphate and 0.2 mg/ml creatine kinase) in import buffer (3% [w/v] bovine serum albumin, 250 mM sucrose, 80 mM KCl, 5 mM $MgCl_2$, 5 mM KP_i, 5 mM methionine and 10 mM MOPS-KOH [pH 7.2]) (Gebert et al., 2011; Ieva et al., 2014). Where indicated, mitochondria were subjected to an in vitro heat shock prior to the import reaction; they were resuspended in import buffer supplemented with 4 mM ATP and incubated for 12–15 min at 37°C. The import was performed at 25°C if not stated differently. For dissipation of $\Delta\psi$, 1 μM valinomycin, 8 μM antimycin A, and 20 μM oligomycin (final concentrations) were added before the import reaction. Where indicated, a treatment with proteinase K (50 μg/ml for 15 min on ice) was performed after the import reaction, followed by the addition of PMSF (1 mM). Subsequently, mitochondria were washed and suspended in SEM buffer. Mitochondria were either solubilized in buffer containing 1% digitonin for blue native electrophoresis or were separated by SDS-PAGE, followed by digital autoradiography.

Protease Accessibility Assay for the Analysis of Membrane Insertion

Hypo-osmotic swelling was induced by 8-fold dilution of mitochondria (in SEM) with EM buffer (10 mM MOPS-KOH [pH 7.2], 1 mM EDTA); control mitochondria received SEM buffer. Where indicated, a treatment with proteinase K (7 μg/ml) or trypsin (8 μg/ml) was performed for 15 min on ice. Trypsin was inactivated by soybean trypsin inhibitor (30-fold excess). Mitochondria were pelleted, washed, and subjected to SDS-PAGE.

Data Analysis

Radiolabeled precursor proteins separated by gel electrophoresis were analyzed by digital autoradiography with the Storm systems 840 and 865, the ImageQuant software (GE Healthcare), the FLA 9000 image scanner and the Multi Gauge software (Fujifilm). Immunoblotting signals were detected using enhanced chemiluminescence and the LAS3000, LAS4000 Imager systems and the Multi Gauge software (Fujifilm). MS data were processed using MaxQuant version 1.3.0.5 and Andromeda. The results were generated and confirmed by using independent biological samples (different mitochondrial

preparations, independent import and assembly experiments). Quantifications of independent assembly experiments (n = 3) are shown as mean ± SEM.

SUPPLEMENTAL INFORMATION

Supplemental Information includes Supplemental Experimental Procedures, four figures, and two tables and can be found with this article at http://dx.doi.org/10.1016/j.cmet.2016.04.005.

AUTHOR CONTRIBUTIONS

S.B.S., J.H., S.O., C.S., S.G.S., J.V.-S., S.E.H., A.E.F., N.G., and M.B. performed experiments and analyzed data together with M.v.d.L., B.W., N.P., and N.W.; J.H.'s contributions include experiments on the sorting of Tim18 and Sdh4 via mtHsp70 and Oxa1 and assembly of the TIM22 complex; S.B.S.'s contributions include experiments on the specificity of *oxa1-ts* effects, membrane insertion of Sdh4, interaction of Sdh4 and Mmt2 with Oxa1, and the identification of different OXA substrates. N.W., N.P., B.W., M.B., and M.v.d.L. designed and supervised the project; S.B.S., J.H., S.O., C.S., and S.G.S. prepared the figures and tables; N.P. and N.W. wrote the manuscript; all authors discussed results from the experiments and commented on the manuscript.

ACKNOWLEDGMENTS

We thank J.M. Herrmann, P. Rehling, and M. Andes for discussion, yeast strains, and basic import experiments and A. Schulze-Specking for expert technical assistance. Work included in this study has also been performed in partial fulfillment of the requirements for the doctoral theses of S.B.S., J.H., and S.G.S. at the University of Freiburg. This work was supported by the Deutsche Forschungsgemeinschaft (PF 202/8-1), the Sonderforschungsbereiche 746 and 1140, the Excellence Initiative of the German federal and state governments (EXC 294 BIOSS; GSC-4 Spemann Graduate School), the European Research Council (ERC) Consolidator Grant Number 648235, the German Academy of Sciences Leopoldina (LPDS 2013-08 to S.E.H.), and a Boehringer Ingelheim Fonds fellowship (to M.B.).

Received: September 5, 2015
Revised: January 2, 2016
Accepted: April 8, 2016
Published: May 10, 2016

REFERENCES

Bohnert, M., Rehling, P., Guiard, B., Herrmann, J.M., Pfanner, N., and van der Laan, M. (2010). Cooperation of stop-transfer and conservative sorting mechanisms in mitochondrial protein transport. Curr. Biol. *20*, 1227–1232.

Bonnefoy, N., Fiumera, H.L., Dujardin, G., and Fox, T.D. (2009). Roles of Oxa1-related inner-membrane translocases in assembly of respiratory chain complexes. Biochim. Biophys. Acta *1793*, 60–70.

Botelho, S.C., Österberg, M., Reichert, A.S., Yamano, K., Björkholm, P., Endo, T., von Heijne, G., and Kim, H. (2011). TIM23-mediated insertion of transmembrane α-helices into the mitochondrial inner membrane. EMBO J. *30*, 1003–1011.

Chacinska, A., Koehler, C.M., Milenkovic, D., Lithgow, T., and Pfanner, N. (2009). Importing mitochondrial proteins: machineries and mechanisms. Cell *138*, 628–644.

Endo, T., and Yamano, K. (2009). Multiple pathways for mitochondrial protein traffic. Biol. Chem. *390*, 723–730.

Funes, S., Nargang, F.E., Neupert, W., and Herrmann, J.M. (2004). The Oxa2 protein of *Neurospora crassa* plays a critical role in the biogenesis of cytochrome oxidase and defines a ubiquitous subbranch of the Oxa1/YidC/Alb3 protein family. Mol. Biol. Cell *15*, 1853–1861.

Funes, S., Kauff, F., van der Sluis, E.O., Ott, M., and Herrmann, J.M. (2011). Evolution of YidC/Oxa1/Alb3 insertases: three independent gene duplications followed by functional specialization in bacteria, mitochondria and chloroplasts. Biol. Chem. *392*, 13–19.

Gebert, N., Gebert, M., Oeljeklaus, S., von der Malsburg, K., Stroud, D.A., Kulawiak, B., Wirth, C., Zahedi, R.P., Dolezal, P., Wiese, S., et al. (2011). Dual function of Sdh3 in the respiratory chain and TIM22 protein translocase of the mitochondrial inner membrane. Mol. Cell *44*, 811–818.

Glick, B.S., Brandt, A., Cunningham, K., Müller, S., Hallberg, R.L., and Schatz, G. (1992). Cytochromes c_1 and b_2 are sorted to the intermembrane space of yeast mitochondria by a stop-transfer mechanism. Cell *69*, 809–822.

Hartl, F.U., Schmidt, B., Wachter, E., Weiss, H., and Neupert, W. (1986). Transport into mitochondria and intramitochondrial sorting of the Fe/S protein of ubiquinol-cytochrome *c* reductase. Cell *47*, 939–951.

Hell, K., Herrmann, J.M., Pratje, E., Neupert, W., and Stuart, R.A. (1998). Oxa1p, an essential component of the N-tail protein export machinery in mitochondria. Proc. Natl. Acad. Sci. USA *95*, 2250–2255.

Hell, K., Neupert, W., and Stuart, R.A. (2001). Oxa1p acts as a general membrane insertion machinery for proteins encoded by mitochondrial DNA. EMBO J. *20*, 1281–1288.

Herrmann, J.M., Neupert, W., and Stuart, R.A. (1997). Insertion into the mitochondrial inner membrane of a polytopic protein, the nuclear-encoded Oxa1p. EMBO J. *16*, 2217–2226.

Hildenbeutel, M., Theis, M., Geier, M., Haferkamp, I., Neuhaus, H.E., Herrmann, J.M., and Ott, M. (2012). The membrane insertase Oxa1 is required for efficient import of carrier proteins into mitochondria. J. Mol. Biol. *423*, 590–599.

Huang, L.S., Shen, J.T., Wang, A.C., and Berry, E.A. (2006). Crystallographic studies of the binding of ligands to the dicarboxylate site of Complex II, and the identity of the ligand in the "oxaloacetate-inhibited" state. Biochim. Biophys. Acta *1757*, 1073–1083.

Ieva, R., Schrempp, S.G., Opaliński, L., Wollweber, F., Höß, P., Heißwolf, A.K., Gebert, M., Zhang, Y., Guiard, B., Rospert, S., et al. (2014). Mgr2 functions as lateral gatekeeper for preprotein sorting in the mitochondrial inner membrane. Mol. Cell *56*, 641–652.

Kumazaki, K., Chiba, S., Takemoto, M., Furukawa, A., Nishiyama, K., Sugano, Y., Mori, T., Dohmae, N., Hirata, K., Nakada-Nakura, Y., et al. (2014). Structural basis of Sec-independent membrane protein insertion by YidC. Nature *509*, 516–520.

Meier, S., Neupert, W., and Herrmann, J.M. (2005). Proline residues of transmembrane domains determine the sorting of inner membrane proteins in mitochondria. J. Cell Biol. *170*, 881–888.

Neupert, W., and Herrmann, J.M. (2007). Translocation of proteins into mitochondria. Annu. Rev. Biochem. *76*, 723–749.

Palmieri, F. (2013). The mitochondrial transporter family SLC25: identification, properties and physiopathology. Mol. Aspects Med. *34*, 465–484.

Park, K., Botelho, S.C., Hong, J., Österberg, M., and Kim, H. (2013). Dissecting stop transfer *versus* conservative sorting pathways for mitochondrial inner membrane proteins *in vivo*. J. Biol. Chem. *288*, 1521–1532.

Park, K., Jung, S.J., Kim, H., and Kim, H. (2014). Mode of membrane insertion of individual transmembrane segments in Mdl1 and Mdl2, multi-spanning mitochondrial ABC transporters. FEBS Lett. *588*, 3445–3453.

Preuss, M., Leonhard, K., Hell, K., Stuart, R.A., Neupert, W., and Herrmann, J.M. (2001). Mba1, a novel component of the mitochondrial protein export machinery of the yeast *Saccharomyces cerevisiae*. J. Cell Biol. *153*, 1085–1096.

Sun, F., Huo, X., Zhai, Y., Wang, A., Xu, J., Su, D., Bartlam, M., and Rao, Z. (2005). Crystal structure of mitochondrial respiratory membrane protein complex II. Cell *121*, 1043–1057.

Wagener, N., Ackermann, M., Funes, S., and Neupert, W. (2011). A pathway of protein translocation in mitochondria mediated by the AAA-ATPase Bcs1. Mol. Cell *44*, 191–202.

Cell Metabolism, Volume *23*

Supplemental Information

Mitochondrial OXA Translocase Plays a Major Role in Biogenesis of Inner-Membrane Proteins

Sebastian B. Stiller, Jan Höpker, Silke Oeljeklaus, Conny Schütze, Sandra G. Schrempp, Jens Vent-Schmidt, Susanne E. Horvath, Ann E. Frazier, Natalia Gebert, Martin van der Laan, Maria Bohnert, Bettina Warscheid, Nikolaus Pfanner, and Nils Wiedemann

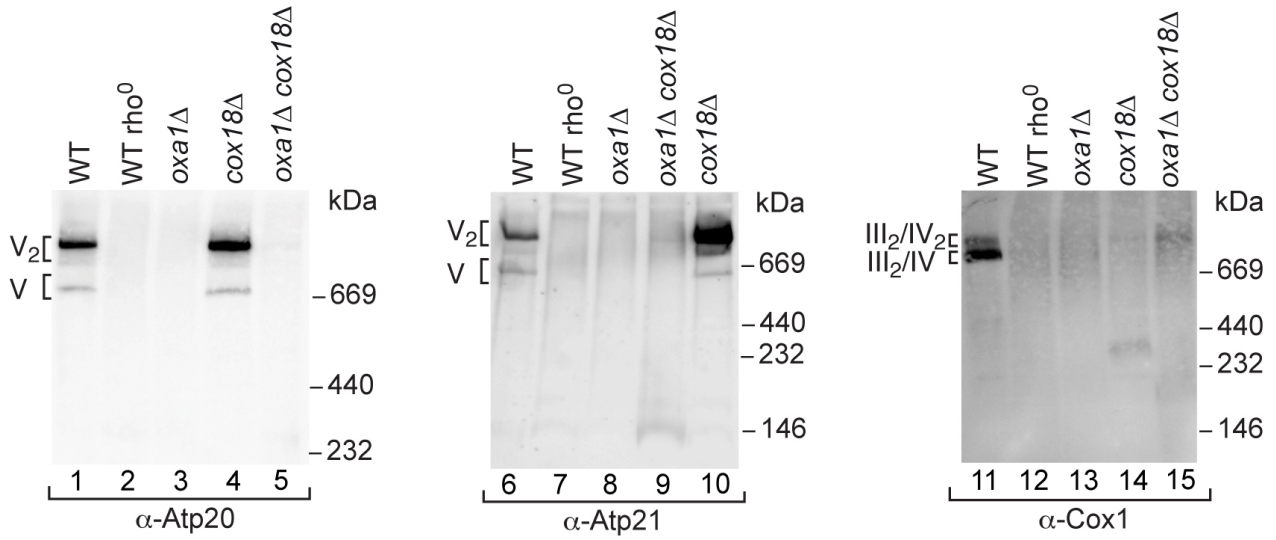

Figure S1. Defects of Oxidative Phosphorylation Complexes in Oxa1-deficient Mitochondria, Related to Figure 1

Mitochondria were isolated from wild-type (WT), WT rho^0, *oxa1*Δ, *cox18*Δ and *oxa1*Δ *cox18*Δ yeast, lysed with digitonin and analyzed by blue native electrophoresis and immunoblotting with the indicated antisera. V, complex V (F_1F_o-ATP synthase); V_2, ATP synthase dimer; III_2/IV and III_2/IV_2, respiratory chain supercomplexes of complex III and complex IV.

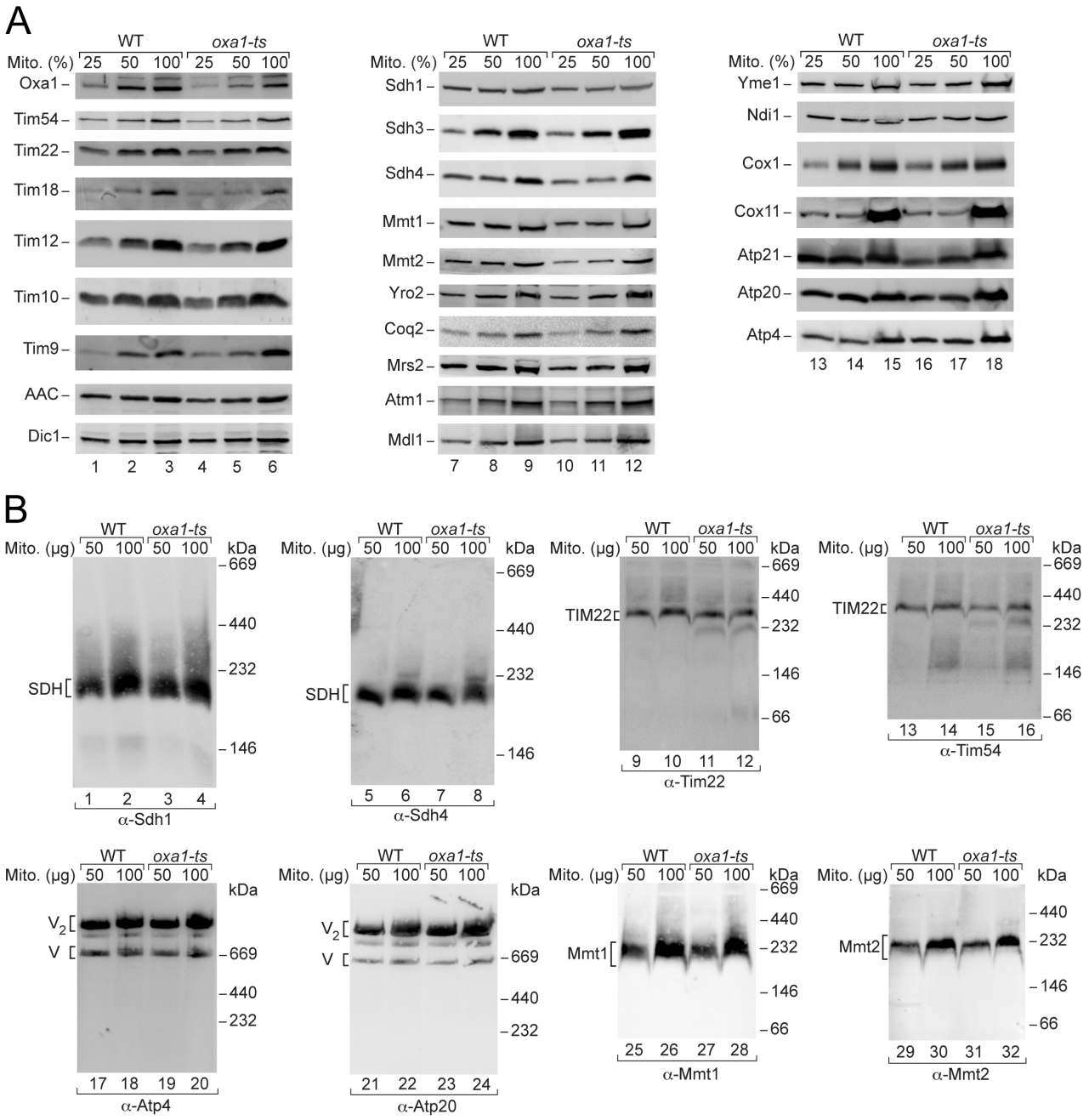

Figure S2. Characterization of Mitochondria Isolated After Growth of *oxa1-ts* Yeast at Permissive Conditions, Related to Figure 2

(A) Wild-type (WT) and *oxa1-ts* yeast cells were grown at 21°C. Mitochondria were isolated and protein levels were analyzed by SDS-PAGE and immunoblotting with antisera against the indicated proteins. Mito., total mitochondrial protein; 100% represents 160 µg protein (80 µg for Tim54, Tim22, Tim12, Tim10, AAC, Dic1, Coq2, Atm1, Mdl1 and Ndi1; 40 µg for Oxa1, Tim9 and Sdh3).

(B) Mitochondria isolated from WT and *oxa1-ts* cells were lysed with 1% digitonin and subjected to blue native electrophoresis and immunoblotting. Without a heat shock, *oxa1–ts* mitochondria have a mild assembly defect, evidenced by a sub-assembled TIM22 complex of ~230 kDa of low abundance (lanes 11, 12, 15 and 16) and reduced levels of the [^{35}S]Tim18-Sdh3 assembly intermediate seen in Figure 2C.

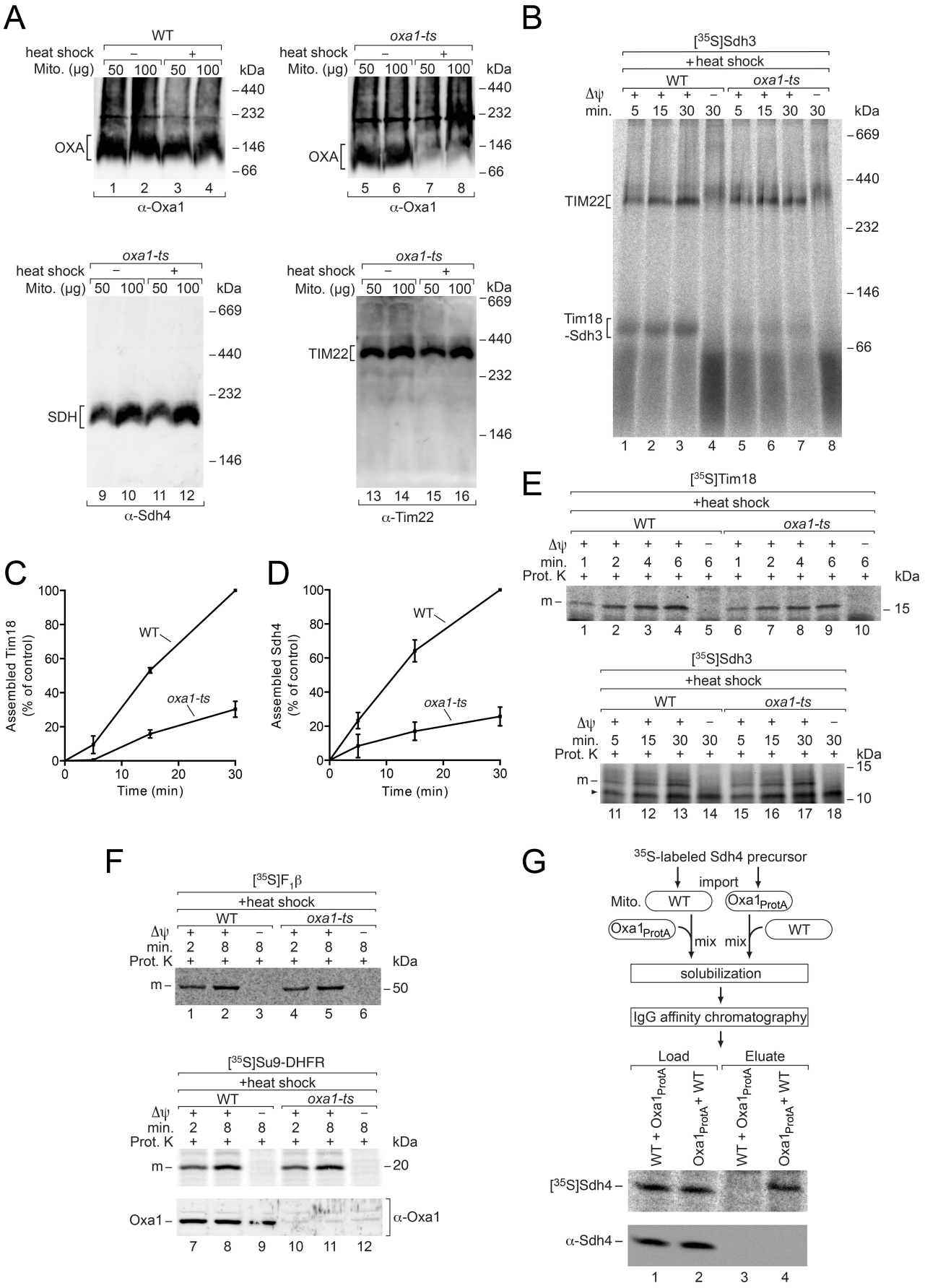
A
WT
oxa1-ts
heat shock
Mito. (µg)
50 100 50 100
kDa
440
232
146
66
OXA
1 2 3 4
α-Oxa1
5 6 7 8
α-Oxa1
669
SDH
9 10 11 12
α-Sdh4
TIM22
13 14 15 16
α-Tim22
B
[35S]Sdh3
+heat shock
Δψ
min.
5 15 30 30 5 15 30 30
TIM22
Tim18
-Sdh3
1 2 3 4 5 6 7 8
C
Assembled Tim18
(% of control)
WT
oxa1-ts
Time (min)
D
Assembled Sdh4
(% of control)
E
[35S]Tim18
Prot. K
m
1 2 3 4 5 6 7 8 9 10
[35S]Sdh3
11 12 13 14 15 16 17 18
F
[35S]F1β
[35S]Su9-DHFR
Oxa1
7 8 9 10 11 12
G
35S-labeled Sdh4 precursor
import
Mito.
Oxa1ProtA
mix
solubilization
IgG affinity chromatography
Load
Eluate
WT + Oxa1ProtA
Oxa1ProtA + WT
[35S]Sdh4
α-Sdh4
1 2 3 4

Figure S3

Figure S3. Characterization of Import and Assembly in *oxa1-ts* Mitochondria, Related to Figure 2

(A) Wild-type (WT) or *oxa1-ts* mitochondria were suspended in import buffer supplemented with 4 mM ATP, followed by either a 12 min heat shock at 37°C or incubation at 25°C. Mitochondria were washed, lysed with digitonin and analyzed by blue native electrophoresis and immunoblotting.

(B) Assembly of Sdh3 in WT and *oxa1-ts* mitochondria. Isolated mitochondria were heat-shocked for 12 min at 37°C. [^{35}S]Sdh3 precursor was imported in the presence of non-radiolabeled Tim18 (Gebert et al., 2011) at 25°C, followed by proteinase K treatment. Formation of the Tim18-Sdh3 assembly intermediate and the TIM22 complex were analyzed by blue native electrophoresis and digital autoradiography. Assembly of [^{35}S]Sdh3 into the TIM22 complex requires the presence of sufficient amounts of Tim18 precursor (supplied in chemical amounts from wheat germ lysate; Gebert et al., 2011). The activity of Oxa1 is rate-limiting for the first assembly step (Tim18-Sdh3 intermediate); [^{35}S]Sdh3 reaching this intermediate is then rapidly assembled into the TIM22 complex.

(C, D) ^{35}S-labeled Tim18 (C) or Sdh4 precursor (D) were imported into in vitro heat-treated (12 min at 37°C) WT and *oxa1-ts* mitochondria at 25°C (C) or 30°C (D). Non-imported precursor was removed by addition of proteinase K. ^{35}S-labeled assembled complexes were analyzed by blue native electrophoresis and quantified by digital autoradiography (mature TIM22 complex (C) or sum of Sdh3-Sdh4 intermediate and mature SDH complex (D)). The assembly yield in WT mitochondria after 30 min import was set to 100% (control). The results are shown as mean ± SEM (n=3 independent experiments; mean with range of two independent experiments for the 15 min time point of (C)).

(E) Radiolabeled Tim18 (lanes 1-10) or Sdh3 precursors (lanes 11-18) were imported into WT and *oxa1-ts* mitochondria at 25°C (Tim18) or 30°C (Sdh3) for the indicated periods. Mitochondria were heat-shocked for 12 min at 37°C before the import reaction. Non-imported precursors were removed by proteinase K. Import was analyzed by SDS-PAGE and autoradiography. m, mature form; arrowhead, unspecific band.

(F) WT and *oxa1-ts* mitochondria were subjected to an in vitro heat shock (37°C) and incubated with the ^{35}S-labeled precursors of $F_1\beta$ (F_1-ATPase subunit β /Atp2) and Su9-DHFR (fusion protein between the presequence of *Neurospora crassa* F_o-ATPase subunit 9 and mouse dihydrofolate reductase) at 25°C, followed by treatment with proteinase K. The mitochondria were analyzed by SDS-PAGE and autoradiography (upper and middle panels) or immunodecoration (lower panel).

(G) [^{35}S]Sdh4 precursor was imported into WT or $Oxa1_{ProtA}$ mitochondria for 8 min at 30°C. After removal of non-imported precursor by proteinase K, [^{35}S]Sdh4-containing mitochondria were mixed with unlabeled mitochondria of the other type as indicated. Mitochondria were solubilized with 1% digitonin and subjected to IgG affinity chromatography, followed by elution with TEV protease. Samples were analyzed by SDS-PAGE and autoradiography (upper panel) or immunodecoration (lower panel). Load 0.15%; eluate 100%. [^{35}S]Sdh4 was only co-purified with tagged Oxa1 when it was imported into $Oxa1_{ProtA}$ mitochondria, excluding a post-lysis interaction of the precursor with $Oxa1_{ProtA}$.

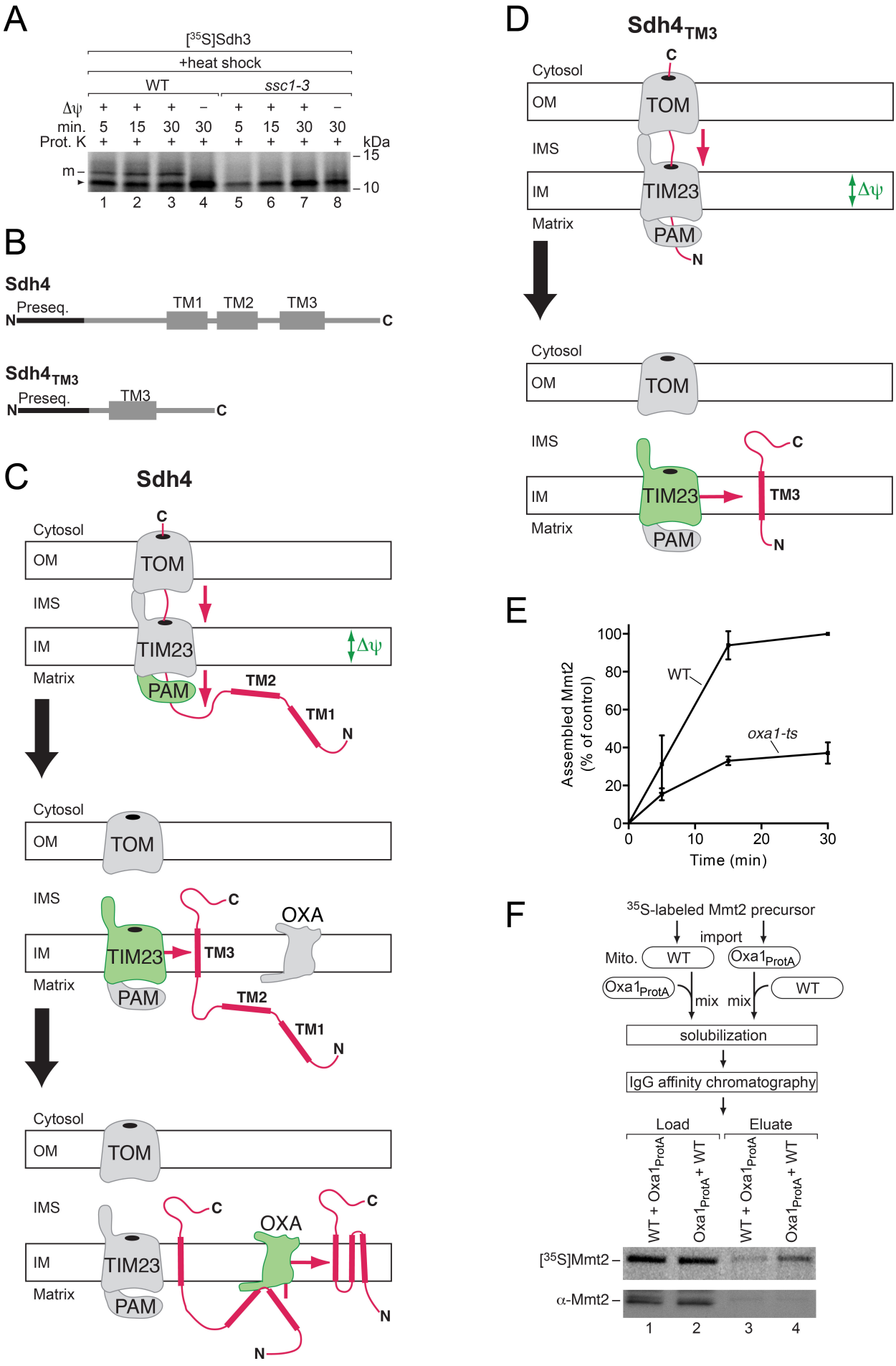
A
[35S]Sdh3
+heat shock
WT
ssc1-3
Δψ + + + − + + + −
min. 5 15 30 30 5 15 30 30
Prot. K + + + + + + + +
kDa
15
10
m
1 2 3 4 5 6 7 8
B
Sdh4
Preseq.
TM1 TM2 TM3
N C
Sdh4TM3
Preseq.
TM3
N C
C
Sdh4
Cytosol
OM
IMS
IM
Matrix
TOM
TIM23
PAM
Δψ
TM2
TM1
N
C
OXA
TM3
D
Sdh4TM3
Cytosol
OM
IMS
IM
Matrix
TOM
TIM23
PAM
Δψ
N
C
TM3
E
Assembled Mmt2 (% of control)
100
80
60
40
20
0
WT
oxa1-ts
0 10 20 30
Time (min)
F
35S-labeled Mmt2 precursor
import
Mito.
WT
Oxa1ProtA
mix
solubilization
IgG affinity chromatography
Load
Eluate
WT + Oxa1ProtA
Oxa1ProtA + WT
[35S]Mmt2
α-Mmt2
1 2 3 4

Figure S4

Figure S4. Import Experiments into Mutant Mitochondria and Hypothetical Model of the Sdh4 Sorting Pathway, Related to Figures 3 and 4

(A) Isolated wild-type (WT) and *ssc1-3* mitochondria were heat-shocked for 12 min at 37°C, followed by import of radiolabeled Sdh3 precursor at 30°C. After removal of non-imported precursor by proteinase K, samples were analyzed by SDS-PAGE and autoradiography. m, mature form; arrowhead, unspecific band.

(B) Scheme of presequence (Preseq.) and transmembrane (TM) segments of Sdh4 and $Sdh4_{TM3}$.

(C, D) Hypothetical model of the mitochondrial sorting pathways of Sdh4 (C) and $Sdh4_{TM3}$ (D). OM, outer mitochondrial membrane; IMS, intermembrane space; IM, inner mitochondrial membrane.

(E) [^{35}S]Mmt2 was imported into in vitro heat-shocked (12 min at 37°C) WT and *oxa1-ts* mitochondria, followed by proteinase K treatment. Mitochondria were analyzed by blue native electrophoresis and Mmt2 assembly was quantified by digital autoradiography. The assembly yield in WT mitochondria after 30 min import was set to 100% (control). The results are shown as mean ± SEM (n=3 independent experiments).

(F) [^{35}S]Mmt2 precursor was imported into WT or $Oxa1_{ProtA}$ mitochondria for 10 min at 30°C and analyzed as described in the legend of Figure S3G, revealing that [^{35}S]Mmt2 was specifically co-purified with tagged Oxa1 only when it was imported into $Oxa1_{ProtA}$ mitochondria.

SUPPLEMENTAL EXPERIMENTAL PROCEDURES

Generation of Yeast Strains and Cloning

Table S2 summarizes the *S. cerevisiae* strains used. Individual chromosomal deletions of *COX18* and *OXA1* were generated by their substitution with a *His3MX6* cassette (Longtine et al., 1998). For chromosomal deletion of the *COX18* gene in *oxa1*Δ yeast, an *URA3* cassette was introduced (Berben et al., 1991). For PCR amplification of integration cassettes, flanked by sequences homologous to the 5' untranslated region (UTR) and 3'-UTR of the selected open reading frame, the KOD Hot Start Master Mix (Merck Millipore) was used. For transformation of yeast strains the lithium acetate/single-stranded carrier DNA/polyethylene glycol method (Gietz and Woods, 2002) was employed and verified by PCR or Western blot analysis. The $Sdh4_{TM3}$ precursor consists of the N-terminal Sdh4 presequence (amino acid residues 1-31 according to Vögtle et al., 2009) followed by the C-terminus of Sdh4 (amino acid residues 121-181). To generate the [^{35}S]Mmt2 precursor, a PCR product encoding amino acid residues 1 to 450 (including presequence and all five TMs) was used.

Plasmids Used in This Study

Name	Backbone	Insert	Source	Number
pGEM-AAC	pGEM-4Z	*S. cerevisiae* AAC2	Wiedemann et al., 2001	1039
pGEM-Dic1	pGEM	BamHI-DIC1 (*S. cerevisiae*)-EcoRI	Pfanner/ Wiedemann Labs	A32
pGEM-Su9-DHFR	pGEM	EcoRI-Su9(1-69, *N. crassa*)-DHFR(mouse)-HindIII	Pfanner/ Wiedemann Labs	SO2
pGEM-$F_1\beta$	pSP64	HindIII-$F_1\beta$ (*S. cerevisiae*)-HindIII	Pfanner/ Wiedemann Labs	F01
YDp-U	pUC9HStop	HindIII-URA3-SmaI	Berben et al., 1991	X45
pFA6a-His3MX6	pFA6	BamHI-P_{TEV}-his5+ (*S. pombe*)-T_{TEV}-EcoRI	Wach, 1996	1424

PCR Primers Used in This Study

Name	Sequence (5'→ 3')	Description
COQ2 SP6 fw	GATCGATTTAGGTGACACTATAGAAGCGGC CACCATGTTTATTTGGCAGAGAAAGAGTATT TTAC	Generation of SP6-Coq2 PCR template for RNA synthesis
COQ2 rev	CTACAAGAATCCAAACAGTCTCAAG	
SP6_Sdh4_f_ SBS	TCGATTTAGGTGACACTATAGAATACGCCGC CGCCGATCTTTCCTACGCTTTCG	Generation of SP6-Sdh4 PCR template for RNA synthesis; generation of SP6-$Sdh4_{TM3}$ construct
Sdh4_rc_SBS	CTACTTCTTGGCTTCAATC	
Sp6Tim18	TCGATTTAGGTGACACTATAGAATACGCCGC CGCCATGCTATTGT	Generation of SP6-Tim18 PCR template for RNA synthesis
Tim18rc	TATGGGTGAGTCAGTTTCTTC	
MMT2 SP6 fw	GATCGATTTAGGTGACACTATAGAAGCGGC CACCATGCTACGGATAAGTATTGACTCTATC	Generation of SP6-Mmt2 PCR template for RNA synthesis
MMT2 rev (Δ451)	TTACATCAACAAACTCGACGTCCAC	
Sdh3_SP6_fwd	TCGATTTAGGTGACACTATAGAATACGCCGC CGCCGCATAGAAATCTCAGGACC	Generation of SP6-Sdh3 PCR template for RNA synthesis
Sdh3_rev	TCATAAAGTTAATAAATAAGTACCGAG	
Sdh4_linker_f	ATTTCTGAAAGAGTTTATGGTG	Generation of SP6-$Sdh4_{TM3}$ construct
Sdh4_linker_rev	CACCATAAACTCTTTCAGAAATGCTCTTCTTA GCGGTAGAC	
Mmt1_RWG_ sense	CTTTAAGAAGGAGATATACCATGTTAAGAAT CTGCGTAAAAAGG	Generation of Mmt1 template DNA using the RTS™ Wheat Germ LinTempGenSet
Mmt1_RWG_anti	TGATGATGAGAACCCCCCCCTCAAATATGAG TATTCGTATGG	
Tim18_RWG_ sense	CTTTAAGAAGGAGATATACCATGCTATTGTTT CCTGGCTTG	Generation of Tim18 template DNA using the RTS™ Wheat Germ LinTempGenSet
Tim18_RWG_ anti	TGATGATGAGAACCCCCCCCTCAGTTTCTTC CAAATATATACAA	
Cox18d_YDp_f2	AAGGTCCAAGGATAGGAAAATTTCAAGATAA AGTATGGCATTGAATTCCCGGGGATCC	Genomic deletion of *COX18* ORF
Cox18d_YDp_r2	CTGATGTAGAATTACATATCCTATCTATGCGT CAGCTTCACGCTAGCTTGGCTGCAG	
Cox18_test_f	CTACCGTCCAGTAATTC	Verification of genomic *COX18* deletion
Cox18_test_r	GTTTATTTACAAGCTGATGTAG	

Mass Spectrometry and Data Analysis

For the SILAC-based quantitative MS analysis of wild-type yeast and an *oxa1 cox18* double deletion strain (*oxa1*Δ *cox18*Δ), equal amounts of Lys8/Arg10-labeled wild-type and non-isotopically labeled mutant cells were mixed based on optical densities before isolation of crude mitochondria. Proteins of the mitochondrial fraction (4 µg protein per LC/MS run) were precipitated with acetone, resuspended in 8 M urea/50 mM NH_4HCO_3, and subjected to reduction with TCEP and alkylation with iodoacetamide followed by

tryptic digestion as described (Lytovchenko et al., 2014). The generated peptides were analyzed by LC/MS using an Ultimate 3000 RSLCnano HPLC system (Thermo Scientific, Dreieich, Germany) directly coupled to an Orbitrap Elite mass spectrometer (Thermo Scientific, Bremen, Germany). Peptides were preconcentrated and washed on a 5 mm x 0.3 mm PepMap™ C18 µ-precolumn (Thermo Scientific) for 25 – 30 min and separated on a 50 cm x 75 µm C18 reversed-phase nano LC column (Acclaim PepMap™ RSLC column; particle size 2 µm; pore size 100 Å; Thermo Scientific) at 40°C using a binary solvent system consisting of 0.1% (v/v) formic acid (solvent A) and 50% (v/v) methanol/30% (v/v) acetonitrile in 0.1% (v/v) formic acid (solvent B). For peptide elution, a linear gradient of 5 – 62% solvent B followed by 62 – 90% solvent B was applied; the flow rate was 250 nl/min. The Orbitrap Elite instrument was operated essentially as described (Hünten et al., 2015).

For protein identification and quantification, mass spectrometric data were processed using MaxQuant (version 1.3.0.5; Cox and Mann, 2008) and Andromeda (Cox et al., 2011) as described (Lytovchenko et al., 2014). The *Saccharomyces* Genome Database (SGD; www.yeastgenome.org) was used for the database search. The option "Re-quantify" implemented in MaxQuant and applied to our data analysis generally allows for the calculation of a SILAC ratio in case a peptide is only present in the isotope-labeled or unlabeled form by assigning a peptide intensity for the missing counterpart from the background signals in MS spectra at the expected *m/z* value. A list of all proteins detected is provided in Table S1.

The presence or absence of a presequence was predicted using TargetP 1.1 (for Atm1 and Nde2) (Emanuelsson et al., 2000; Nielsen et al., 1997) or evaluated according to Vögtle et al. (2009) (for Mdl2, Mmt2, Coq2, Sdh3, Sdh4, Cox15 and Pam17), Vukotic et al. (2012) (for Rcf2) and Bohnert et al. (2015) (for Mic10). Transmembrane segments were predicted by using TMpred (Hofmann and Stoffel, 1993).

Analysis of Proteins Using SDS-PAGE and Blue Native Electrophoresis

For separation of proteins using Tricine-SDS-PAGE, 10-16.5% discontinuous polyacrylamide gels (1 M Tris-HCl [pH 8.45], 0.1% [w/v] SDS) were employed using cathode buffer (100 mM Tris, 100 mM Tricine, 0.1% [w/v] SDS [pH 8.25]) and anode buffer (200 mM Tris-HCl [pH 8.9]). Alternatively, the non-polymerized separating gel (16%/6 M urea) was overlaid with 10% gel (w/o glycerol) that, after polymerization, was covered with a 4% sample gel (AB-6) (Schägger, 2006). For protein separation using the Tris-glycine buffer system, 12% or 16% discontinuous polyacrylamide gels were employed (Laemmli, 1970).

Steady state protein levels of mitochondria were analyzed by lysis of 10–320 µg of mitochondria (protein amount) with Laemmli buffer (2% [w/v] SDS, 10% [v/v] glycerol, 60

mM Tris-HCl [pH 6.8], 0.01% [w/v] bromphenol blue, 1% [v/v] β-mercaptoethanol, 1 mM PMSF) followed by electrophoretic separation and Western blotting onto polyvinylidene fluoride membranes. Protein levels were determined using immunodecoration with enhanced chemiluminescence (Haan and Behrmann, 2007).

For blue native electrophoresis, 6–16.5% or 3–13% discontinuous polyacrylamide gels (50 mM Bis Tris-HCl [pH 7.0], 67 mM ε-amino n-caproic acid) were used for separation (cathode buffer: 50 mM Tricine [pH 7.0], 15 mM Bis-Tris, (0.02% [w/v] Coomassie G); anode buffer: 50 mM Bis-Tris-HCl [pH 7.0]). For the analysis of steady state levels of protein complexes, 50–100 µg of mitochondria (protein amount) were solubilized in 1% digitonin buffer (1% [w/v] digitonin, 20 mM Tris-HCl [pH 7.4], 0.1 mM EDTA, 50 mM NaCl, 10% [v/v] glycerol, 1 mM PMSF) and incubated for 15 min on ice. After removal of non-solubilized material by centrifugation, blue native loading dye was added (final concentration: 0.5% [w/v] Coomassie G-250, 50 mM ε-amino n-caproic acid, 100 mM Bis-Tris-HCl [pH 7.0]) and the samples were loaded onto the blue native gel. After the running front had migrated into the running gel, the cathode buffer was exchanged with the buffer without Coomassie G (Schägger and von Jagow, 1991; Schägger et al., 1994).

IgG Affinity Chromatography

Radiolabeled Sdh4 or Mmt2 precursor was imported into 1.2 mg (protein amount) of wild-type (WT, YPH499) or $Oxa1_{ProtA}$ mitochondria for 8–10 min at 30°C. Non-imported precursor was digested with proteinase K. Mitochondria were pelleted and the supernatant was discarded. To remove residual traces of radioactive precursor proteins, mitochondria were resuspended in SEM buffer and subjected to another clarifying spin. Subsequently WT or $Oxa1_{ProtA}$ mitochondria were mixed with 1.2 mg of untreated mitochondria of the other type. The mitochondrial mixture was solubilized in 2 ml of solubilization buffer (20 mM Tris-HCl [pH 7.4], 50 mM NaCl, 0.1 mM EDTA, 10% [v/v] glycerol, 1% [w/v] digitonin, 1.5 mM PMSF, 1x EDTA-free Protease Inhibitor Cocktail [Roche]). Non-solubilized material was pelleted by centrifugation and a portion of the soluble fraction was taken as load. 100 µl of 50% slurry human IgG-coupled Sepharose beads were equilibrated with solubilization buffer and added to solubilized mitochondria followed by 90 min head-over-head incubation at 4°C. Beads were transferred to a mobicol column and washed 15-times with 500 µl of wash buffer (20 mM Tris-HCl [pH 7.4], 60 mM NaCl, 0.5 mM EDTA, 10% [v/v] glycerol, 0.3% [w/v] digitonin, 1.5 mM PMSF, 1x EDTA-free Protease Inhibitor Cocktail [Roche]). Proteins specifically bound to IgG beads via $Oxa1_{ProtA}$ were eluted by incubation with tobacco etch virus (TEV) protease under vigorous shaking at 4°C overnight. Samples were subjected to SDS-PAGE and Western Blotting followed by autoradiography and antibody decoration.

Antibodies Used in This Study

Antigen	Dilution	Number	Secondary antibody
Aac2	1:500 TBS-T + 5% milk	GR3617-7	anti-rabbit
Atm1	1:200 TBS-T + 5% milk	GR1641-7	anti-rabbit
Atp4	1:500 TBS-T + 5% milk	GR1970-4	anti-rabbit
Atp20	1:500 TBS-T + 5% milk	GR1516-4	anti-rabbit
Dic1	1:200 TBS-T + 5% milk	GR2054-5	anti-rabbit
Coq2	1:50 TBS	GR2097; affinity purified e1-e9	anti-rabbit
Cox1	1:400 TBS-T + 5% milk	GR1538-4	anti-rabbit
Cox11	1:200 TBS-T + 5% milk	GR1102-2	anti-rabbit
Mdl1	1:200 TBS-T + 5% milk	GR1518-7	anti-rabbit
Mdj2	1:400 TBS-T + 5% milk	GR1842-7	anti-rabbit
Mia40	1:750 TBS-T + 5% milk	B315	anti-rabbit
Mir1	1:1000 TBS-T + 5% milk	171-5	anti-rabbit
Mmt1	1:50 TBS	GR2049; affinity purified e1-e6	anti-rabbit
Mmt2	1:25 TBS	GR2090; affinity purified ++	anti-rabbit
Mrs2	1:25 TBS	GR2093; affinity purified e5-e8	anti-rabbit
Ndi1	1:200 TBS-T + 5% milk	GR809-4	anti-rabbit
Oxa1	1:100 TBS-T + 5% milk	262-6	anti-rabbit
Sam50	1:300 TBS-T + 5% milk	B312-14	anti-rabbit
Sdh1	1:1000 TBS-T + 5% milk	GR1849-3	anti-rabbit
Sdh3	1:250 TBS-T + 5% milk	GR2434-5	anti-rabbit
Sdh4	1:2000 TBS-T + 5% milk	GR1855-3	anti-rabbit
Pam16	1:200 TBS-T + 5% milk	GR750-6	anti-rabbit
Tim9	1:250 TBS-T + 5% milk	GR2013-5	anti-rabbit
Tim10	1:500 TBS-T + 5% milk	217-8	anti-rabbit
Tim11/ Atp21	1:400 TBS-T + 5% milk	138-9	anti-rabbit
Tim12	1:250 TBS-T + 5% milk	GR906-7	anti-rabbit
Tim13	1:1000 TBS-T + 5% milk	238-5	anti-rabbit
Tim18	1:1000 TBS-T + 5% milk	233-7	anti-rabbit
Tim22	1:500 TBS-T + 5% milk	164-4	anti-rabbit
Tim23	1:500 TBS-T + 5% milk	133-9	anti-rabbit
Tim50	1:500 TBS-T + 5% milk	257-8	anti-rabbit
Tim54	1:1000 TBS-T + 5% milk	215-6	anti-rabbit
Tom40	1:750 TBS-T + 5% milk	168-4	anti-rabbit
Yme1	1:400 TBS-T + 5% milk	GR1435-3	anti-rabbit
Yro2	1:200 TBS-T + 5% milk	GR2095-4	anti-rabbit

SUPPLEMENTAL REFERENCES

Berben, G., Dumont, J., Gilliquet, V., Bolle, P.A., and Hilger, F. (1991). The YDp plasmids: a uniform set of vectors bearing versatile gene disruption cassettes for *Saccharomyces cerevisiae*. Yeast *7*, 475–477.

Bohnert, M., Zerbes, R.M., Davies, K.M., Mühleip, A.W., Rampelt, H., Horvath, S.E., Boenke, T., Kram, A., Perschil, I., Veenhuis, M., et al. (2015). Central role of Mic10 in the mitochondrial contact site and cristae organizing system. Cell Metab. *21*, 747–755.

Cox, J., and Mann, M. (2008). MaxQuant enables high peptide identification rates, individualized p.p.b.-range mass accuracies and proteome-wide protein quantification. Nature Biotechnol. *26*, 1367–1372.

Cox, J., Neuhauser, N., Michalski, A., Scheltema, R.A., Olsen, J.V., and Mann, M. (2011). Andromeda: a peptide search engine integrated into the MaxQuant environment. J. Proteome Res. *10*, 1794–1805.

Emanuelsson, O., Nielsen, H., Brunak, S., and von Heijne, G. (2000). Predicting subcellular localization of proteins based on their N-terminal amino acid sequence. J. Mol. Biol. *300*, 1005–1016.

Frazier, A.E., Dudek, J., Guiard, B., Voos, W., Li, Y., Lind, M., Meisinger, C., Geissler, A., Sickmann, A., Meyer, H.E., et al. (2004). Pam16 has an essential role in the mitochondrial protein import motor. Nat. Struct. Mol. Biol. *11*, 226–233.

Frazier, A.E., Taylor, R.D., Mick, D.U., Warscheid, B., Stoepel, N., Meyer, H.E., Ryan, M.T., Guiard, B., and Rehling, P. (2006). Mdm38 interacts with ribosomes and is a component of the mitochondrial protein export machinery. J. Cell Biol. *172*, 553–564.

Gambill, B.D., Voos, W., Kang, P.J., Miao, B., Langer, T., Craig, E.A., and Pfanner, N. (1993). A dual role for mitochondrial heat shock protein 70 in membrane translocation of preproteins. J. Cell Biol. *123*, 109–117.

Gietz, R.D., and Woods R.A. (2002). Transformation of yeast by lithium acetate/single-stranded carrier DNA/polyethylene glycol method. Methods Enzymol. *350*, 87–96.

Haan, C., and Behrmann, I. (2007). A cost effective non-commercial ECL-solution for Western blot detections yielding strong signals and low background. J. Immunol. Methods *318*, 11–19.

Hofmann, K., and Stoffel, W. (1993). TMBASE – A database of membrane spanning protein segments. Biol. Chem. Hoppe-Seyler *374*, 166.

Hünten, S., Kaller, M., Drepper, F., Oeljeklaus, S., Bonfert, T., Erhard, F., Dueck, A., Eichner, N., Friedel, C.C., Meister, G., et al. (2015). p53-regulated networks of protein, mRNA, miRNA, and lncRNA expression revealed by integrated pulsed stable isotope labeling with amino acids in cell culture (pSILAC) and next generation sequencing (NGS) analyses. Mol. Cell. Proteomics *14*, 2609–2629.

Laemmli, U.K. (1970). Cleavage of structural proteins during the assembly of the head of bacteriophage T4. Nature *227*, 680–685.

Longtine, M.S., McKenzie, A. 3rd, Demarini, D.J., Shah, N.G., Wach, A., Brachat, A., Philippsen, P., and Pringle, J.R. (1998). Additional modules for versatile and economical PCR-based gene deletion and modification in *Saccharomyces cerevisiae*. Yeast *14*, 953–961.

Lytovchenko, O., Naumenko, N., Oeljeklaus, S., Schmidt, B., von der Malsburg, K.,

Deckers, M., Warscheid, B., van der Laan, M., and Rehling, P. (2014). The INA complex facilitates assembly of the peripheral stalk of the mitochondrial F_1F_o-ATP synthase. EMBO J. *33*, 1624–1638.

Nielsen, H., Engelbrecht, J., Brunak, S., and von Heijne, G. (1997). Identification of prokaryotic and eukaryotic signal peptides and prediction of their cleavage sites. Protein Eng. *10*, 1–6.

Schägger H. (2006). Tricine-SDS-PAGE. Nat. Protoc. *1*, 16–22.

Schägger, H., and von Jagow, G. (1991). Blue native electrophoresis for isolation of membrane protein complexes in enzymatically active form. Anal. Biochem. *199*, 223–231.

Schägger, H., Cramer, W.A., and von Jagow, G. (1994). Analysis of molecular masses and oligomeric states of protein complexes by blue native electrophoresis and isolation of membrane protein complexes by two-dimensional native electrophoresis. Anal. Biochem. *217*, 220–230.

Sikorski, R.S., and Hieter, P. (1989). A system of shuttle vectors and yeast host strains designed for efficient manipulation of DNA in *Saccharomyces cerevisiae*. Genetics *122*, 19–27.

Thomas, B.J., and Rothstein, R. (1989). Elevated recombination rates in transcriptionally active DNA. Cell *56*, 619–630.

Vögtle, F.N., Wortelkamp, S., Zahedi, R.P., Becker, D., Leidhold, C., Gevaert, K., Kellermann, J., Voos, W., Sickmann, A., Pfanner N., et al. (2009). Global analysis of the mitochondrial N-proteome identifies a processing peptidase critical for protein stability. Cell *139*, 428–439.

Vukotic, M., Oeljeklaus, S., Wiese, S., Vögtle, F.N., Meisinger, C., Meyer, H.E., Zieseniss, A., Katschinski, D.M., Jans, D.C., Jakobs, S., et al. (2012). Rcf1 mediates cytochrome oxidase assembly and respirasome formation, revealing heterogeneity of the enzyme complex. Cell Metab. *15*, 336–347.

Wach, A. (1996). PCR-synthesis of marker cassettes with long flanking homology regions for gene disruptions in *S. cerevisiae*. Yeast *15*, 259–265.

Wiedemann, N., Pfanner, N., and Ryan, M.T. (2001). The three modules of ADP/ATP carrier cooperate in receptor recruitment and translocation into mitochondria. EMBO J. *20*, 951–960.

Table S1. Proteins Identified in Mitochondrial Fractions by Quantitative MS-Based Analysis of Wild-Type Versus *oxa1 cox18* Double Deletion Yeast (see Excel File), Related to Figure 1

Table S2. Yeast Strains Used in This Study, Related to Figures 1, 2 and 3

Strain	Description	Genotype	Source	Number
Wild-type (WT)	YPH499	*MAT*a *ura3-52 lys2-801 ade2-101 trp1-Δ63 his3-Δ200 leu2-Δ1*	Sikorski and Hieter, 1989	1501
Wild-type (WT)	W303-1A *MAT*a; WT for *oxa1-ts* strain	*MAT*a *leu2-3,112 trp1-1 can1-100 ura3-1 ade2-1 his3-11,15*	Thomas and Rothstein, 1989	1045
Wild-type (WT)	YPH499; *pam16::ADE2* pFL39-PAM16; WT for *pam16-3*	YPH499 *pam16::ADE2* pFL39-PAM16	Frazier et al., 2004	3156
Wild-type (WT)	PK82; WT for *ssc1-3* (PK83)	*MATα his4-713 lys2 ura3-52 leu2-3,112 Δtrp1*	Gambill et al., 1993	2501
Wild-type rho^0	YPH499 rho^0; devoid of mitochondrial DNA; generated by ethidium bromide treatment	*MAT*a *ura3-52 lys2-801 ade2-101 trp1-Δ63 his3-Δ200 leu2-Δ1; rho^0*	Pfanner/ Wiedemann Labs	1519
*oxa1*Δ	Deletion of *OXA1* in YPH499 cells	YPH499 *oxa1*::*HIS3MX6*	This study (A.E. Frazier and P. Rehling)	1474
*cox18*Δ	Deletion of *COX18* in YPH499 cells (deletion of ORF (1-951) and 20 base pairs downstream of ORF)	YPH499 *cox18*::*HIS3MX6*	This study (A.E. Frazier and P. Rehling)	1526
*oxa1*Δ *cox18*Δ	Deletion of *OXA1* and *COX18* in YPH499 cells	YPH499 *oxa1::HIS3MX6 cox18::URA3*	This study	3754
oxa1-ts	*oxa1^{ts}* (L240S)	W303-1A *MAT*a *oxa1::OXA1^{L240S}*	Hell et al., 2001; Preuss et al., 2001	2277
Oxa1$_{ProtA}$	Oxa1$_{ProtA}$ (chromosomal)	YPH499 *oxa1*:: *OXA1ProtAHIS3MX6*	Frazier et al., 2006	1522
ssc1-3	PK83	*MATα ade2-101 lys2 ura3-52 leu2-3,112 Δtrp1 ssc1-3(LEU2)*	Gambill et al., 1993	2503
pam16-3	Chromosomal deletion of *PAM16* complemented with temperature-sensitive *pam16-3* allele on plasmid	YPH499 *pam16::ADE2 pFL39-PAM16ts-3*	Frazier et al., 2004	3158